

1 **Analogue experiments on releasing and restraining bends and their**  
2 **application to the study of the Barents Shear Margin**

3  
4  
5  
6 **Roy H. Gabrielsen<sup>1</sup>, Panagiotis A. Giannenas<sup>2</sup>, Dimitrios Sokoutis<sup>1,3,4</sup>,**  
7 **Ernst Willingshofer<sup>3,4</sup>, Muhammad Hassaan<sup>1,4</sup> & Jan Inge Faleide<sup>1</sup>**

8  
9 <sup>1</sup>Department of Geosciences, University of Oslo, Norway

10 <sup>2</sup>[panagiotis-athanasios.giannenos@univ-rennes1.fr](mailto:panagiotis-athanasios.giannenos@univ-rennes1.fr)

11 <sup>3,4</sup>Faculty of Geosciences, Utrecht University, the Netherlands

12 <sup>4</sup>Vår Energi AS, Grundingen 3, 0250 Oslo, Norway

13  
14  
15 **Corresponding author: Roy H. Gabrielsen ([r.h.gabrielsen@geo.uio.no](mailto:r.h.gabrielsen@geo.uio.no))**

16  
17 **ORCI-id:**

18 Jan Inge Faleide: 0000-0001-8032-2015

19 Roy H. Gabrielsen: 0000-0001-5427-8404

20 Muhammad Hassaan: 0000-0001-6004-8557

21  
22  
23  
24  
25 **Abstract:**

26 The Barents Shear Margin separates the Svalbard and Barents Sea from the North  
27 Atlantic. ~~It includes one northern (Hornsund Fault Zone) and a southern (Senja~~  
28 ~~Fracture Zone) margin segment in which structuring was dominated by dextral~~  
29 ~~shear. These segments are separated by the Vestbakken Volcanic Province that~~  
30 ~~rests in a releasing bend position between the two.~~ During the break-up of the  
31 North Atlantic the plate tectonic configuration was characterized by sequential  
32 dextral shear, extension, and finally contraction and inversion. This generated a  
33 complex zone of deformation that contains several structural families of over-  
34 lapping and reactivated structures. ~~Although the convolute structural pattern~~  
35 ~~associated with the Barents Shear Margin has been noted, it has not yet been~~  
36 ~~explained in this framework.~~

37 A series of crustal-scale analogue experiments, utilizing a scaled stratified sand-  
38 silicon polymer sequence ~~were utilized in the, serve to~~ study ~~of~~ the structural  
39 evolution of the shear margin. ~~in response to shear deformation along a pre-~~  
40 ~~defined boundary representing the geometry of the Barents Shear Margin and~~  
41 ~~variations in kinematic boundary conditions of subsequent deformation events,~~  
42 ~~i.e. direction of extension and inversion. 1)The experiments reproduced the~~  
43 ~~geometry and positions of the major basins and relations between structural~~  
44 ~~elements (fault and fold systems) as observed along and adjacent to the Barents~~  
45 ~~Shear Margin. This supports the present structural model for the shear margin.~~

46  
47 The most significant observations ~~that are~~ of particular significance for  
48 interpreting the structural configuration of the Barents Shear Margin are:

49 ~~1)The experiments reproduced the geometry and positions of the major basins~~  
50 ~~and relations between structural elements (fault and fold systems) as observed~~

51 ~~along and adjacent to the Barents Shear Margin. This supports the present~~  
52 ~~structural model for the shear margin.~~

53 ~~13) Prominent early-stage positive structural elements (e.g. folds, push-ups)~~  
54 ~~interacted with younger (e.g. inversion) structures and contributed to a hybrid~~  
55 ~~complex-final structural pattern.~~

56 2) Several of the structural features that were initiated during the early (dextral  
57 shear) stage became overprinted and obliterated in the subsequent stages.

58 ~~3) Prominent early stage positive structural elements (e.g. folds, push ups)~~  
59 ~~interacted with younger (e.g. inversion) structures and contributed to a complex~~  
60 ~~final structural pattern.~~

61 34) All master faults, pull-part basins and extensional shear duplexes initiated  
62 during the shear stage quickly became linked in the extension stage, generating a  
63 connected basin system along the entire shear margin at the stage of maximum  
64 extension.

65 45) The fold pattern generated during the terminal stage (contraction/inversion  
66 became dominant in the basinal areas and was characterized by fold axes with  
67 traces striking parallel to the basin margins. These folds, however, most strongly  
68 affected the shallow intra-basinal layers.

69 The experiments reproduced the geometry and positions of the major basins and  
70 relations between structural elements (fault and fold systems) as observed along  
71 and adjacent to the Barents Shear Margin. This supports the present structural  
72 model for the shear margin.

73  
74 ~~This is in general agreement with observations in previous and new reflection~~  
75 ~~seismic data from the Barents Shear Margin.~~

#### 76 77 **Plain language summary:**

78 The Barents Shear Margin defines the border between the relatively shallow  
79 Barents Sea that is situated on a continental plate, and the deep ocean. The margin  
80 is characterized by a complex structural pattern that has resulted from the  
81 opening and separation of the continent and the ocean, starting c. 655 million  
82 years ago. This history included one phase of right-lateral shear and one phase of  
83 ~~spreading~~oblique extension, the latter including a subphase of shortening,  
84 perhaps due to plate tectonic reorganizations. The area has been mapped by the  
85 study of reflection seismic lines for decades, but many details of its development  
86 is not yet fully constrained. We therefore ran a set of scaled experiments to  
87 investigate what kind of structures could be expected in this kind of tectonic  
88 environment, and to figure out what is a reasonable time relation between them.  
89 From these experiments we deduced several types of structures-/faults, folds and  
90 sedimentary basins) that helps us to improve the understanding of the history of  
91 the opening of the North Atlantic.

92  
93  
94 **Key words:** Analogue experiments, dextral strike-slip, releasing and restraining  
95 bends, multiple folding, Barents Shear Margin, basin inversion

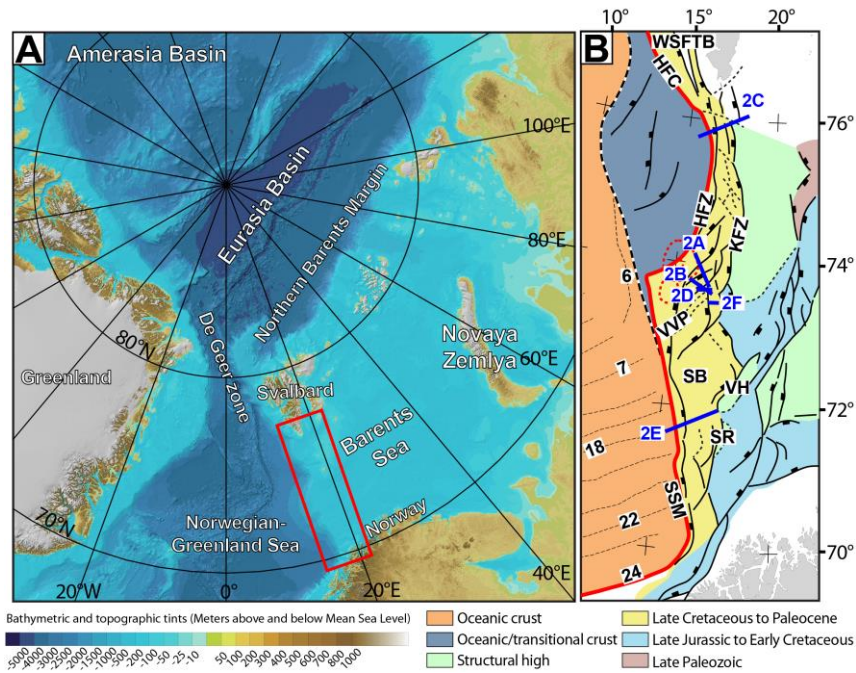
96  
97

98 **Introduction**

99  
100 Physiography, width and structural style of the Norwegian continental margin  
101 vary considerably along its strike (e.g. Faleide et al., 2008, 2015). The margin  
102 includes a southern rifted segment between 60° and 70°N and a northern sheared-  
103 rifted segment between 70° and 82°N (**Figure 1A**). The latter coincides with the  
104 ocean-ward border of the western Barents Sea and Svalbard margins (e.g. Faleide  
105 et al., 2008) and is referred to here as “the Barents Shear Margin”. This segment  
106 coincides with the continent-ocean transition (COT) of the northernmost part of  
107 the North Atlantic Ocean, and its configuration is typical for that of transform  
108 margins where the structural pattern became established in an early stage of  
109 shear, later to develop into an active continent-ocean passive margin (Masclé &  
110 Blarez, 1987; Lorenzo, 1997; Seiler et al., 2010; Basile, 2015; Nemcok et al., 2016).  
111 ~~Late Cretaceous~~—Palaeogene shear, rifting, breakup and incipient spreading in  
112 the North Atlantic was associated with voluminous magmatic activity, resulting in  
113 the development of the North Atlantic Volcanic Province (Saunders et al., 1997;  
114 Ganerød et al., 2010; Horni *et al.*, 2017). According to its tectonic development, the  
115 Barents Shear Margin (**Figure 1B**) incorporates, or is bordered by, several distinct  
116 structural elements, some of which are associated with volcanism and halokinesis.

117  
118 The multistage development combined with a complex geometry caused  
119 interference between structures (and sediment systems) in different stages of the  
120 margin development. Such relations are not always obvious, but interpretation  
121 can be supported by the help of scaled ~~experiments-models~~. In combining the  
122 interpretation of reflection seismic data and analogue modeling, therefore, we  
123 investigate structures generated in (initial) dextral shear, the development into  
124 seafloor spreading and subsequent contraction in this process, the later stages of  
125 which were likely influenced by plate reorganization (Talwani & Eldholm, 1977;  
126 Gaina et al., 2009; ~~see also~~ see also Vågnes et al., 1998; Pascal & Gabrielsen, 2001;  
127 Pascal et al., 2005; Gac et al., 2016) ~~and/or~~ other far-field stresses (Doré & Lundin,  
128 1996; Lundin & Doré, 1997; Doré et al., 1999; 2016; Lundin et al., 2013). The  
129 present experiments were designed to illuminate the structural complexity  
130 affiliated with multistage sheared passive margins, so that the significance of

131 structural elements like fault and fold systems observed along the Barents Shear  
 132 Margin could be set



133  
 134 **Figure 1: A)** The Barents Sea provides is separated from the Norwegian-  
 135 Greenland Sea by the De Geer Zone linking the North Atlantic to the Arctic Eurasia  
 136 Basin. Red box shows the present study area. **B)** Structural map Barents Sea shear  
 137 margin. Note segmentation of the continent-ocean transition. Abbreviations (from  
 138 north to south): WSFTB = West Spitsbergen Fold-and-Thrust Belt, HFZ =  
 139 Hornsund Fault Zone, KFZ = Knølegga Fault Zone, VVP = Vestbakken Volcanic  
 140 Province, SB = Sørvestsnaget Basin, VH = Veslemøy High, SR = Senja Ridge, SSM =  
 141 Senja Shear Margin. Blue lines indicate position of seismic profiles in Figure 2 and  
 142 red line in Figure 1B shows the western limitation of the thinned crust (see also  
 143 Figure 3). Chron numbers are indicated on oceanic crust area.  
 144

145 into a dynamic context. [The study area suffered repeated and contrasting stages](#)  
 146 [of deformation, including dextral shear, oblique extension, inversion and volcanic](#)  
 147 [activity. This is a particular challenge in such tectonic settings, that are](#)  
 148 [characterized by repeated overprinting and canabalization of -incipient by](#)  
 149 [younger structural elements. The experimental approach opens for the](#)  
 150 [identification and characterisation of the different stages of deformation and their](#)  
 151 [affiliated structural elements on the way to the present-day margin geometry.](#)

152  
153  
154  
155  
156  
157  
158  
159  
160  
161  
162  
163  
164  
165  
166  
167  
168  
169  
170  
171  
172  
173  
174  
175  
176  
177  
178  
179  
180  
181  
182  
183  
184

### Regional ~~setting~~background

In the following sections we provide definitions and a short description of the most important structural elements constituting the study area. ~~The structural elements are presented in-sequence from north to south and All structural elements described below are displayed in~~ (Figure 1B).

~~The greater Barents Shear Margin is a part of the preceeding and more extensive~~was preceded by the “De Geer Zone” ~~megashear system which linked the Norwegian Greenland Sea and the Arctic Eurasia Basin system~~ -(Eldholm et al., 1987; 2002; Faleide et al., 1988; Breivik et al., 1998; 2003). Together with its conjugate Greenland counterpart it carries the evidence of an extensive period of structural ~~developmenting~~, starting with post-Caledonian (Devonian) extension and culminating with ~~PalaeogeneCenozoic~~ break-up of the North Atlantic (e.g., Brekke, 2000; Gabrielsen et al., 1990; Faleide et al., 1993; 2008; Gudlaugsson et al., 1998; ~~Tsikalas et al., 2012~~). Two shear margin segments that are separated by a central rift-dominated segment can be identified in the Barents Shear Margin (Myhre et al., 1982; Vågnes, 1997; Myhre & Eldholm, 1988; Ryseth et al., 2003; Faleide at al., 1988; 1993; 2008). Each segment maintained a particular signature concerning the structural and magmatic characteristics of the crust during its development. Of these the Senja Shear Margin is the southernmost segment, originally termed the Senja Fracture Zone by Eldholm et al., (1987). ~~Particularly the hanging wall west of the Knølegga Fault Complex of the Barents Shear Margin was affected by wrench deformation as seen from several push-ups and fold systems (Grogan et al., 1999; Bergh & Grogan 2003).~~ Here, NNW-SSE-striking folds interfere with folds with NE-SW-striking axes ~~(Giennenas, 2018)~~. Strain partitioning may also have affected some of the other shear zone segments of the study area (~~Sørvestsnaget Basin~~; Kristensen et al., 2017). ~~Shearing contributed to the development of releasing and restraining bends, associated pull-apart-basins, neutral strike-slip segments, flower-structures and fold-systems (sensu Crowell, 1974 a,b; Biddle & Christie-Blick, 1985a,b; Cunningham & Mann, 2007a,b).~~ ~~Particularly the hanging wall west of the Knølegga Fault Complex (see below) of~~

Formatted: Font: Not Bold

Formatted: Font: Not Bold

Formatted: Font: Not Bold

Formatted: Font: Not Bold

Formatted: English (United States)

185 the Barents Shear Margin was affected by wrench deformation as seen from  
186 several push-ups and fold systems (Grogan et al., 1999; Bergh & Grogan 2003).

187  
188 The Hornsund Fault Zone and West Spitsbergen Fold-and Thrust Belt form  
189 the northernmost segment of the Barents Shear Margin and coincide with the  
190 northern continuation of the De Geer Zone and the Senja Shear Margin. The  
191 presently distinguishable master fault of this system is the Hornsund Fault Zone,  
192 which together with the West Spitsbergen fold-and-thrust-belt provides a type  
193 setting for transpression and strain partitioning (Harland, 1965; 1969; 1971;  
194 Lowell, 1972; Gabrielsen et al., 1992; Maher et al., 1997; Leever et al., 2011 a,b).  
195 Plate tectonic reconstructions suggest that the plate boundary accommodated c.  
196 750 km along-strike displacement and 20-40 km of shortening in the Eocene  
197 (Bergh et al., 1997; Gaina et al., 2009).

198  
199 The Knølegga Fault Zone Complex can be seen as a part of the Hornsund fault  
200 system extending from the southern tip of Spitsbergen (Gabrielsen et al., 1990). It  
201 trends NNE-SSW to N-S and defines the western margin of the Stappen High. The  
202 vertical displacement approaches 6 km, being the cumulative effect of several  
203 phases of faulting throughout Late Paleozoic, Mesozoic and Cenozoic times.  
204 Although the main movements along the fault may be Tertiary of age, it is likely  
205 that it was initiated much earlier. The Tertiary-Cenozoic displacement may have  
206 had a lateral (dextral) component (Gabrielsen et al., 1990).

207  
208 The Vestbakken Volcanic Province is the central topic of the present  
209 contribution. It represents the rifted segment of the Senja-Barents Shear Margin  
210 and links the sheared margin segments that are situated to the north and south of  
211 it and occupies a typical right-double (eastward) stepping (eastward)-releasing-  
212  bend-setting. Prominent volcanoes and sill-intrusions display significant  
213 magmatic activity, and three distinct volcanic events are distinguished in the  
214 Vestbakken Volcanic Province (Jebsen & Faleide, 1998; Faleide et al., 2008; Libak  
215 et al., 2012). The area has been affected by complex tectonics and both extensional  
216 and contractional structures are observed. The Vestbakken Volcanic Province is  
217 delineated towards the east by an extensional top-west fault zone that parallels

218 the Knølegga Fault Complex). The interior of the Vestbakken Volcanic Province is  
219 dominated by NE-SW-striking extensional faults and associated fault blocks.  
220 Positive structural elements include inverted fault blocks, and wide-angle ( $\lambda > 20$   
221 km) anticlines (roll-over anticlines?) and domes that are overprinted by faults and  
222 folds with amplitudes and wavelengths on the hundred- and km-scales.  
223  
224 The ~~e~~Eastern ~~b~~Boundary ~~f~~Fault (EBF) is a top-west normal fault with a regional  
225 NNE-SSW strike, consisting of two separate, linked segments. Its northern  
226 segment dips more steeply to the WNW than the southern segment. The total  
227 vertical displacement as measured on the early Eocene level is in the order of 300  
228 m~~see~~ (450 m), and the upper part of the hanging wall displays a normal drag  
229 modified by hanging wall tight anticline suggesting post--early Miocene inversion.  
230 Several normal, dominantly NE-SW-striking NW-facing normal faults transect the  
231 hanging wall of the ~~EBF~~-fault. The Central Fault (CF) is the ~~most~~  
232 ~~prominent~~~~largest~~ of those and is hard-linked to the central segment of the ~~EBF~~-  
233 ~~fault is the largest of those. The Central Fault is the most prominent fault of a NW-~~  
234 ~~SE striking fault population that characterizes the entire Vestbakken Volcanic~~  
235 ~~Province.~~All other faults in this map are secondary faults, mainly acting as  
236 accommodation structures to the master faults. Starting from the southern part of  
237 the area and south of the well site, a population of secondary faults is expressed  
238 as anastomosing faults traces.  
239  
240 ~~Three~~Two main episodes of Cenozoic extensional faulting were identified in the  
241 Vestbakken Volcanic Province: (i) a late Paleocene-early Eocene event, which  
242 correlates in time with ~~the~~ continental break-up in the Norwegian-Greenland Sea,  
243 and (ii) an early Oligocene event is tentatively correlated to plate reorganization  
244 around 34 Ma activating~~ed~~ mainly NE-SW striking faults, and (iii) an extensional  
245 ~~Pliocene~~ event. Evidence of volcanic activity coincide with ~~both~~the first two of  
246 these events. Additional extensional events are recorded in mid-Eocene, late  
247 Oligocene and early Miocene times (Jebsen, 1998). The Vestbakken Volcanic  
248 Province is constrained to its east by the eastern boundary fault (EBF in **Figure**  
249 **1B**), that is a part of the Knølegga Fault ~~Zone~~~~Complex~~, separating the Vestbakken  
250 Volcanic Province from the marginal Stappen High further to the east (Blaich et

251 [al., 2017](#)). To the south and southeast the Vestbakken Volcanic Province drops  
252 gradually into the Sørvestsnaget Basin across the southern extension of the  
253 eastern boundary fault and its associated faults. To the west and north the area is  
254 delineated by the continent--ocean boundary/transition. ~~The Vestbakken~~  
255 ~~Volcanic Province includes both extensional and contractional structures (eg.~~  
256 ~~Jebesen & Faleide, 1998; Faleide et al., 2008; Blaich et al., 2017). All other faults in~~  
257 ~~this map are secondary faults, mainly acting as accommodation structures to the~~  
258 ~~master faults. Starting from the southern part of the area and south of the well site,~~  
259 ~~a population of secondary faults is expressed as anastomosing faults traces.~~

260  
261 **The Sørvestsnaget Basin** occupies the area east of the COT between 71 and 73°N  
262 and is characterized by an exceptionally thick Cretaceous-Cenozoic sequence  
263 (Gabrielsen et al., 1990). To the west it is delineated by the Senja Shear Margin  
264 and to the northeast it is separated from the Bjørnøya Basin by the southern part  
265 of the Knølegga Fault Complex (Faleide et al., 1988). The position of the Senja  
266 Ridge coincides with southeastern border of the Sørvestsnaget Basin (Figure 1B),  
267 whereas the Vestbakken Volcanic Province is situated to its north. An episode of  
268 Cretaceous rifting in the Sørvestsnaget Basin seems to have climaxed in the  
269 Cenomanian-middle Turonian (Breivik et al., 1998) to become succeeded by Late  
270 Cretaceous-Palaeocene fast sedimentation (Ryseth et al., 2003). Particularly the  
271 later stages of the basin development were strongly influenced by the opening of  
272 the North Atlantic (Hanisch, 1984; Brekke & Riis, 1987). Salt diapirism did also  
273 contribute to structuring of this basin (Perez-Garcia et al., 2013).

274  
275  
276 **The Senja Ridge** runs parallel to the continental margin and coincides with the  
277 western border of the Tromsø Basin. It is characterized by a N-S-trending gravity  
278 anomaly which are interpreted as buried mafic-ultramafic intrusions which are  
279 associated with the Seiland Igneous Province (Fichler & Pastore, 2022). The  
280 structural development of the Senja Ridge has been associated with shear  
281 affiliated with the development of the shear margin (Riis et al., 1986).

282

Formatted: Font: Not Bold

283 **The Senja Shear Margin** was active during the Eocene opening of the Norwegian-  
284 Greenland Sea during dextral shear that was accompanied by splitting out slivers  
285 of continental crust that became isolated units embedded by oceanic crust during  
286 seafloor spreading (Faleide et al., 2008). The Senja Shear Margin coincides with  
287 the western margin of a basin system that is characterized by significant crustal  
288 thinning and extreme sedimentary thicknesses of that may approach 18-20 km.  
289 This part of the shear margin was characterized by a composite architecture even  
290 at the earliest stages of its development (Faleide et al., 2008). ~~Subsequently~~  
291 ~~shearing contributed to the development of releasing and restraining bends,~~  
292 ~~associated pull apart basins, neutral strike slip segments, flower structures and~~  
293 ~~fold systems (sensu Crowell, 1974 a,b; Biddle & Christie-Blick, 1985a,b;~~  
294 ~~Cunningham & Mann, 2007a,b). Particularly the hanging wall west of the Knølogga~~  
295 ~~Fault Complex (see below) of the Barents Shear Margin was affected by wrench~~  
296 ~~deformation as seen from several push-ups and fold systems (Grogan et al., 1999;~~  
297 ~~Bergh & Grogan 2003).~~ The structural development of the **Senja Shear**  
298 ~~m~~**Margin** was complicated by active halokinesis in the Sørvestsnaget Basin  
299 (Knutsen & Larsen, 1997; Gudlaugsson et al., 1998; Ryseth et al., 2003).

300  
301 ~~The Hornsund Fault Zone and West Spitsbergen Fold and Thrust Belt form~~  
302 ~~the northernmost segment of the Barents Shear Margin and coincides with the~~  
303 ~~northern continuation of the De Geer Zone and the Senja Shear Margin. The~~  
304 ~~presently distinguishable master fault of this system is the Hornsund Fault Zone,~~  
305 ~~which together with the West Spitsbergen fold and thrust belt provides a~~  
306 ~~classical setting for transpression and strain partitioning (Harland, 1965; 1969;~~  
307 ~~1971; Lowell, 1972; Gabrielsen et al., 1992; Maher et al., 1997; Leever et al., 2011~~  
308 ~~a,b). Plate tectonic reconstructions suggest that the plate boundary~~  
309 ~~accommodated c. 750 km along-strike displacement and 20-40 km of shortening~~  
310 ~~in the Eocene (Bergh et al., 1997; Gaina et al., 2009).~~

311  
312 ~~The Sørvestsnaget Basin~~ occupies the area east the COT between 71 and 73°N  
313 and is characterized by an exceptionally thick Cretaceous-Cenozoic sequence  
314 (Gabrielsen et al., 1990). To the west it is delineated by the Senja Shear Margin  
315 and to the northeast it is separated from the Bjørnøya Basin by the southern part

316 of the Knølegga Fault Complex (Faleide et al., 1988). The Senja Ridge coincides  
317 with its southeastern border, whereas the Vestbakken Volcanic Province is  
318 situated to its north. An episode of Cretaceous rifting in the Sørvestsnaget Basin  
319 seems to have climaxed in the Cenomanian-middle Turonian (Breivik et al., 1998)  
320 to become succeeded by Late Cretaceous-Palaeocene fast sedimentation (Ryseth  
321 et al., 2003). Particularly the later stages of the basin development were likely  
322 strongly influenced by the opening of the North Atlantic (Hanisch, 1984; Brekke &  
323 Riis, 1987). Salt diapirism did also contribute to structuring of this basin (Perez-  
324 Garcia et al., 2013).

325  
326 **The Senja Ridge** runs parallel to the continental margin and coincides with the  
327 western border of the Tromsø Basin. It is characterized by a N-S-trending gravity  
328 anomaly which are interpreted as buried mafic-ultramafic intrusions which are  
329 associated with the Seiland Igneous Province (Fichler & Pastore 2022). The  
330 structural development of the Senja Ridge has been linked to shear affiliated with  
331 the development of the shear margin (Riis et al. 1986).

332  
333 ~~**The Knølegga Fault Complex** can be seen as a part of the Hornsund fault system~~  
334 ~~extending from the southern tip of Spitsbergen (Gabrielsen et al., 1990). It trends~~  
335 ~~NNE-SSW to N-S and defines the western margin of the Stappen High. The vertical~~  
336 ~~displacement approaches 6 km. Although the main movements along the fault may~~  
337 ~~be Tertiary of age, it is likely that it was initiated much earlier. The Tertiary~~  
338 ~~displacement may have had a lateral (dextral) component (Gabrielsen et al,~~  
339 ~~1990).~~

340  
341 ~~**The Vestbakken Volcanic Province** is the central topic of the present~~  
342 ~~contribution. It represents the rifted segment of the Senja Shear Margin and links~~  
343 ~~the sheared margin segments that are situated to the north and south of it and~~  
344 ~~occupies a typical right double stepping (eastward) releasing bend setting.~~  
345 ~~Prominent volcanoes and sill intrusions display significant magmatic activity, and~~  
346 ~~three distinct volcanic events are distinguished in the Vestbakken Volcanic~~  
347 ~~Province (Jebsen & Faleide, 1998; Faleide et al., 2008; Libak et al., 2012). The area~~  
348 ~~has been affected by complex tectonics and both extensional and contractional~~

349 structures are observed. The Vestbakken Volcanic Province is delineated towards  
350 the east by an extensional top-west fault zone that parallels the Knølegga Fault  
351 Complex). The interior of the Vestbakken Volcanic Province is dominated by NE-  
352 SW-striking extensional faults and associated fault blocks. Positive structural  
353 elements include inverted fault blocks, and wide-angle ( $\lambda > 20$  km) anticlines (roll-  
354 over anticlines?) and domes that are overprinted by faults and folds with  
355 amplitudes and wavelengths on the hundred- and km-scales.

356 The eastern boundary fault (EBF) is a top-west normal fault with a regional NNE-SSW  
357 strike, consisting of two separate, hard-linked segments. Its northern segment dips  
358 more steeply to the WNW than the southern segment. The total vertical displacement  
359 as measured on the early Eocene level is in the order of 300 msec (450m), and the upper  
360 part of the hanging wall displays a normal drag modified by hanging wall tight anticline  
361 suggesting post early Miocene inversion. Several normal, dominantly NE-SW striking  
362 NW-facing normal faults transect the hanging wall of the EBF fault. The Central Fault  
363 (CF) is the largest of those and is hard-linked to the central segment of the EBF fault is  
364 the largest of those. The Central Fault is the most prominent fault of a NW-SE striking  
365 fault population that characterizes the entire Vestbakken Volcanic Province. Three  
366 episodes of Cenozoic extensional faulting were identified in the Vestbakken  
367 Volcanic Province: (i) a late Paleocene-early Eocene event, which correlates in  
368 time with the continental break-up in the Norwegian-Greenland Sea, (ii) an early  
369 Oligocene event is tentatively correlated to plate reorganization around 34 Ma  
370 activated mainly NE-SW striking faults and (iii) an extensional Pliocene event.  
371 Evidence of volcanic activity coincide with the first two of these events. The  
372 Vestbakken Volcanic Province is constrained to its east by the eastern boundary  
373 fault (EBF in **Figure 1B**), that is a part of the Knølegga Fault Complex, separating  
374 the Vestbakken Volcanic Province from the marginal Stappen High further to the  
375 east. To the south and southeast the Vestbakken Volcanic Province drops  
376 gradually into the Sørvestsnaget Basin across the southern extension of the  
377 eastern boundary fault and its associated faults. To the west and north the area is  
378 delineated by the continent-ocean boundary/transition (marked as COB in Fig.  
379 4.1). The Vestbakken Volcanic Province includes both extensional and  
380 contractional structures (e.g. Jebson & Faleide, 1998; Faleide et al., 2008; Blaiçh et  
381 al., 2017). Cenozoic tectonic activity has left its imprint at the eastern part of the

382 ~~study area. All other faults in this map are secondary faults, mainly acting as~~  
383 ~~accommodation structures to the master faults. Starting from the southern part of~~  
384 ~~the area and south of the well site, a population of secondary faults is expressed~~  
385 ~~as anastomosing faults traces.~~

### 387 **Reflection seismic dData and structural interpretation**

Formatted: Font: +Body (Cambria)

388  
389 The data set of this study includes 2D seismic reflection data from several surveys  
390 and well data in the Vestbakken Volcanic Province. Data coverage is less dense in  
391 northern part of the study area. Typical spacing of seismic lines is 4 km. Well  
392 7316/5-1 was used to correlate the seismic data with formation tops in the study  
393 area whereas published paper based correlations provided calibration and age of  
394 each seismic horizon mapped (e.g. Eidvin et al., 1993; 1998; Ryseth et al., 2003).  
395 Three stratigraphic groups are present in the well; the Nordland Group (473 - 945  
396 m); the Sotbakken Group (945-3752m) and Nygrunnen Group (3752-4014m)  
397 (Eidvin et al., 1993; 1998; [www.npd.com](http://www.npd.com)).

Formatted: Font: +Body (Cambria)

Field Code Changed

Formatted: Font: +Body (Cambria)

Formatted: Font: +Body (Cambria)

### 399 **Fold families**

400 ~~Several folds of regional significance and (with axial traces that can be followed~~  
401 ~~along strike for 2-3 km or more) occur in the Vestbakken Volcanic Province. The~~  
402 ~~folds commonly are situated in the hanging walls of extensional faults and the fold~~  
403 ~~traces and the structural grain of the thick-skinned master faults are generally~~  
404 ~~parallel. This shows that the position and orientation of the folds were determined~~  
405 ~~by the preexisting structural fabric affiliated with these faults, some of which bear~~  
406 ~~the characteristics of tectonic inversion. The fold axial traces parallel the fault~~  
407 ~~traces or are situated in the strike continuation of such. It therefore seems obvious~~  
408 ~~that the structural grain, as defined by the thick skinned master faults strongly~~  
409 ~~influenced the positions of the subsequent folds. The continuity of these~~  
410 ~~foldstructures~~ remains obscure due to spacing of reflection seismic lines, so each  
411 fold may include undetected overlap zones or axial off-sets that have not been  
412 detected. The folds were identified on the lower Eocene, Oligocene and lower  
413 Miocene levels. All the mapped folds are either positioned in the hanging walls of

Formatted: Font: +Body (Cambria)

414 extensional (sometimes inverted) master faults or are dissected by younger faults  
415 with minor throws.

416

417 ~~Three basic fold families were identified in the Vestbakken Volcanic Province by~~  
418 ~~Giennenas (2018): Fold family 1 (Figure 2) consists of gentle to open anticline-syncline~~  
419 ~~pairs with upright to slightly inclined axial planes, sometimes with shallowly plunging~~  
420 ~~fold axes and saddle points, so that the folds are not strictly cylindrical. Folds of this~~  
421 ~~family strikes dominantly NE-SW to NNE-SSW and are generally situated at some~~  
422 ~~distance from the master basin margin faults and in the central parts of the Vestbakken~~  
423 ~~Volcanic Province where larger faults are less abundant. The wavelengths are in the~~  
424 ~~order of 3-10 km and the amplitudes may reach 400 m. The fold flanks sometimes~~  
425 ~~display smaller open folds with wavelengths on the hundred meter scale that may be~~  
426 ~~parasitic, whereas the central parts are commonly broken by post folding steep brittle~~  
427 ~~normal faults that define separate fault zones that are separate from the major folds~~  
428 ~~along strike (see Fold family 3 below). Fold family 2 includes folds with inclined axial~~  
429 ~~planes with dominantly long NW limbs and short SE limbs (Figure 2), which are more~~  
430 ~~common along the basin margin and in affiliation with low angle intra-basin reverse~~  
431 ~~faults. These generally have the characteristics of fault propagation folds and are~~  
432 ~~positioned in the hanging walls with steep, inverted normal faults. These are~~  
433 ~~characterized of axial planes with dips of up to 45 deg) and snake head geometries~~  
434 ~~commonly found in the hanging walls of master faults (Figure 2A, B). Fold family~~  
435 ~~includes anticline-syncline pairs with fold axes that are parallel and are situated more~~  
436 ~~distally to the eastern boundary fault (EBF) and are found internally in extensional fault~~  
437 ~~blocks. The fold axes of the latter sub-family have up right axial planes and are~~  
438 ~~accordingly generally oriented N-S~~

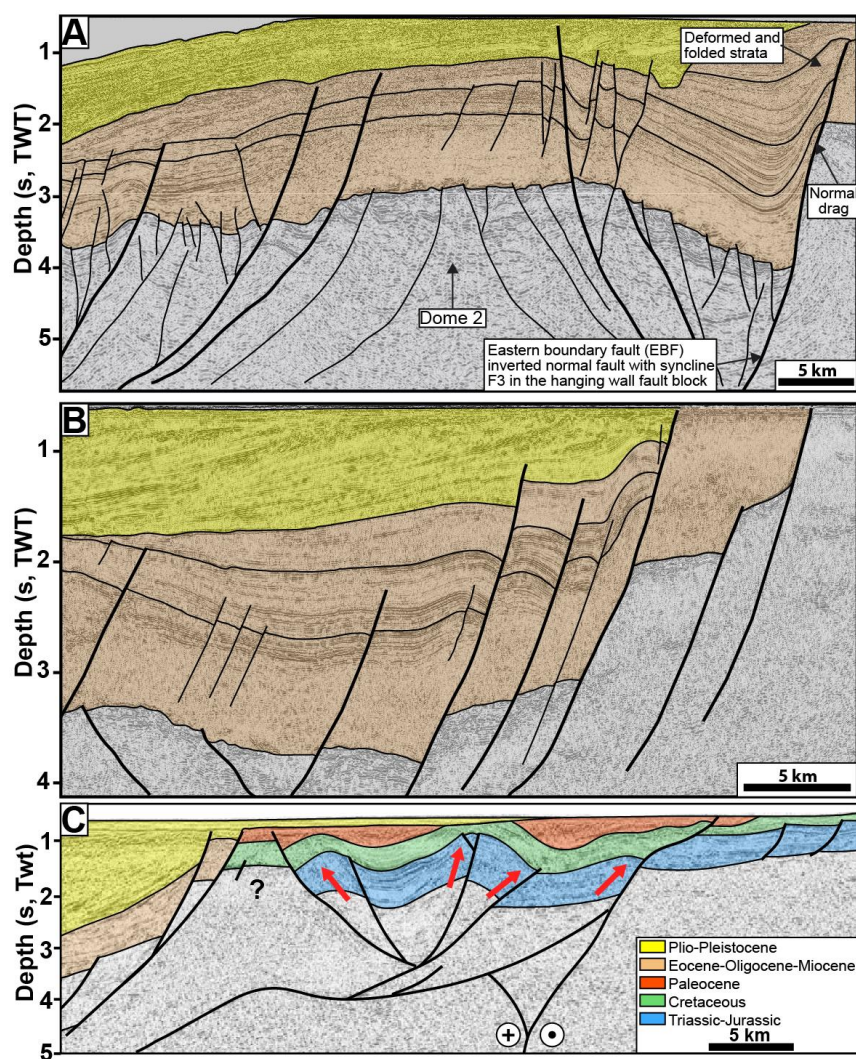
439

## 440 **Strike-slip systems and analogue shear experiments**

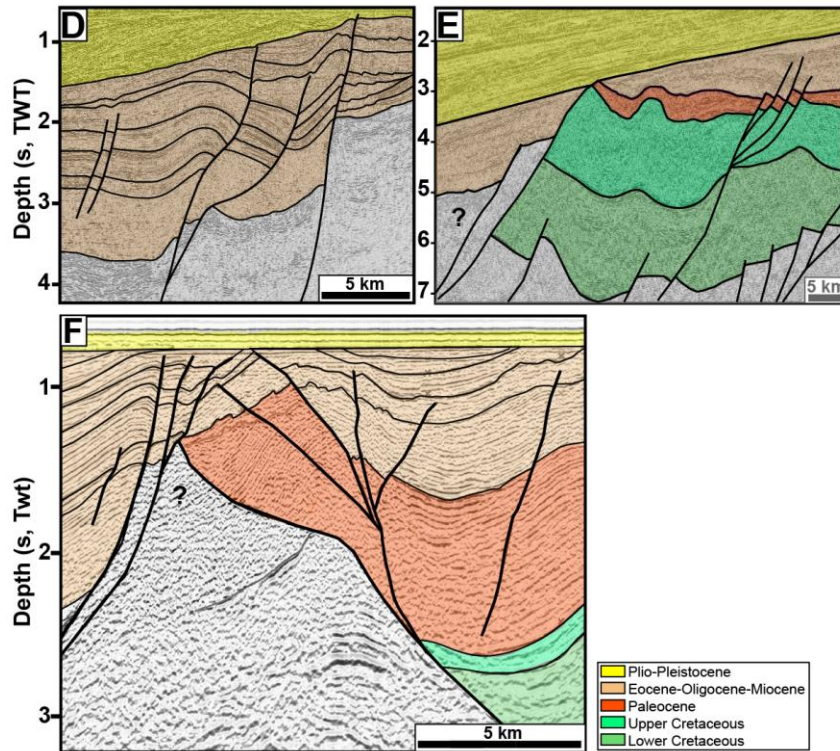
441

442 Shear margins and strike-slip systems are structurally complex and highly  
443 dynamic, ~~so that the eventual architecture of such systems include structural~~  
444 ~~elements that were not contemporaneous meaning that the incipient and mature~~  
445 ~~stages of strike-slip deformation commonly display a variety of geometries (e.g.,~~  
446 ~~Graymer et al., 2007, ) making it hard to comprehend the full complexity solely~~

447 through fieldwork (e.g. Crowell, 1962; 1974a,b; Woodcock & Fischer, 1986;  
 448 Mousloupoulou et al., 2007; 2008). Analogue models offer the option to study the  
 449 dynamics of such relations illustrate such complexity well and therefore attracted  
 450 the attention of early workers in this field (e.g. Cloos 1928; Riedel 1929) and have  
 451 continued to do so until today. Early experimental works mostly utilized one-layer  
 452 ("Riedel-box") models (e.g. Emmons 1969; Tchalenko, 1970; Wilcox et al., 1973),  
 453 which were soon to be expanded by the study of multilayer systems (e.g. Faugère  
 454 et al., 1986; Naylor et al., 1986; Richard et al.,



455



456

457 **Figure 2:** Seismic examples from various segments of the Barents Sea shear margin. **A)** Gentle, partly collapsed NE-SW-striking anticline/dome in the eastern  
 458 terrace domain of the southern Vestbakken Volcanic Province. The origin of this  
 459 structure is obscure, but one can speculate that some of the open syncline-  
 460 anticline pairs originated as PSE-1-structures. **B)** Flower (PSE-2)-structure in area  
 461 dominated by neutral shear. **C)** Section through push-up (PSE-4-structure)  
 462 associated with restraining bend. **D-E)** Asymmetrical folds situated along the  
 463 eastern margin of the Vestbakken Volcanic Province, representing primary PSE-  
 464 5-structures. These structures are focused in the hangingwalls along the  
 465 escarpments of master fault blocks. **F)** Trains of symmetrical folds with upright  
 466 fold axes (PSE-6-structure family) are preserved inside larger fault blocks. See  
 467 Table 1 and text for explanation of the PSE-structures.  
 468  
 469

470 1991; Richard & Cobbold, 1989, 1995; Schreurs, 1994, 2003; Manduit & Dauteuil,  
 471 1996; Dateuil & Mart, 1998; Schreurs & Colletta, 1998, 2003; Ueta et al., 2000;  
 472 Dooley & Schreurs, 2012). The systematics and dynamics of strike-slip systems  
 473 have been focused upon in a number of summaries like Sylvester (1985; 1988);  
 474 Biddle & Christie-Blick (1985a,b); Cunningham & Mann (2007); Dooley &  
 475 Schreurs (2012); Nemcok et al. (2016) and Peacock et al. (2016). Concepts and

476 **Table 1**  
 477 Characteristics of Positive Structural Elements (PSE-1 -PSE-6) as described in text and shown in figures. Note that PSE-1-structures that  
 478 were developed in the earliest stages of the experiments became cannibalized or obliterated during the continued deformation. No  
 479 candidates of this structure population were identified with certainty in reflection seismic sections.  
 480

Struct. type	Structural configuration	Orientation	Expr. stage	Segment	Recognized in seismic	Figure Expr	Figure Seism
<b>PSE-1</b>	Open syn-anticline system	135 deg	Stage 1	1,3	?	5,6	1A?
<b>PSE-2</b>	Incipient flower or half-flower	Parallel master fault	Stage 1	1,2,3	Yes	5,6,8	1B
<b>PSE-3</b>	Forced folds above rotated fault blocks	Parallel master fault in releasing bend	Stage 2	1,2	Yes	9B	
<b>PSE-4</b>	Push-up	Parallel master fault in restraining bend	Stage 1	2	Yes	9D	1C
<b>PSE-5</b>	Anticlines/snake-heads in hanging walls	Parallel master faults	Stage 3	1,2,3	Yes	9C,D	1D,E
<b>PSE-6</b>	Anticline-syncline trains	Parallel master faults	Stage 3	1,2,3	Yes	12	1F

481

482 nomenclature established in these works are used in the following descriptions  
483 and analysis. Also, following Christie-Blick & Biddle (1985a,b) and Dooley &  
484 Schreurs (2012) we apply the term Principal Deformation Zone (PDZ) for the  
485 junction between the movable polythene plates underlying the experiment. The  
486 contact between the fixed and movable base defined a non-stationary velocity  
487 discontinuity ("VD"; Ballard et al., 1987; Allemand & Brun, 1991; Tron & Brun,  
488 1991).

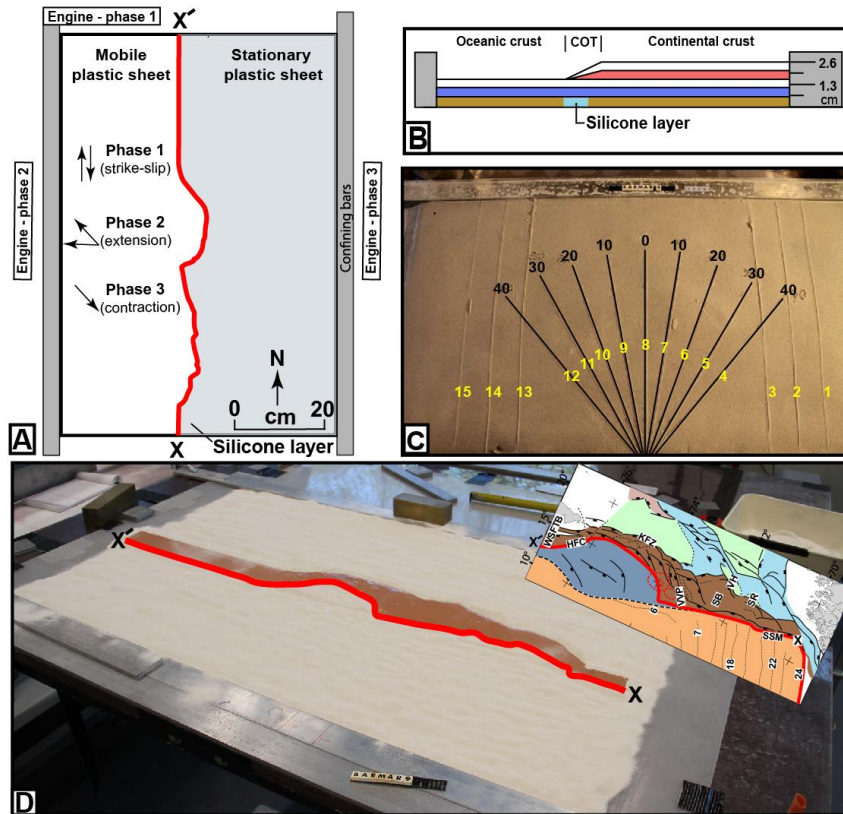
489  
490 Several experimental [studiesworks](#) have particularly focused on the geometry and  
491 development of pull-apart-basins in releasing bend settings (Mann et al., 1983;  
492 Faugère et al. 1983; Richard et al. 1995; Dooley & McClay 1997; Basile & Brun  
493 1999; Sims et al., 1999; Le Calvez & Vendeville, 2002; Mann, 2007; Mitra & Paul,  
494 2011). The pull-apart basin was described by Burchfiel & Stewart (1966) and  
495 Crowell (1974a,b) as formed at a releasing bend or at a releasing fault step-over  
496 along a strike-slip zone (Biddle & Christie-Blick 1985a,b). This basin type has also  
497 been termed "rhomb grabens" (Freund, 1971) and "strike-slip basins" (Mann et  
498 al., 1993) and is commonly considered to be synonymous with the extensional  
499 strike-slip duplex (Woodcock & Fischer, 1986; Dooley & Schreurs, 2012). In the  
500 descriptions of our experiments, we found it convenient to distinguish between  
501 extensional strike-slip duplexes in the context of Woodcock & Fischer (1986) and  
502 Twiss & Moores, 2007, p. 140-141;) and pull-apart basins (rhomb grabens:  
503 Crowell, 1974a,b; Aydin & Nur, 1993) since they reflect slightly different stages in  
504 the development in our experiments (see discussion).

505

## 506 **Experimental setup**

507

508 To study the kinematics of complex shear margins, a series of analogue  
509 experiments were performed at the tectonic modelling laboratory (TecLab) of  
510 Utrecht University, The Netherlands. All experiments were built on two  
511 overlapping 1 mm thick plastic sheets (each 100 cm long and 50 cm wide) that  
512 were placed on a flat, horizontal table surface. The boundary between the  
513 underlying movable and overlaying stationary plastic sheets had the shape of the  
514 mapped continent-ocean boundary (COB; **Figure 1B**). The moveable sheet was

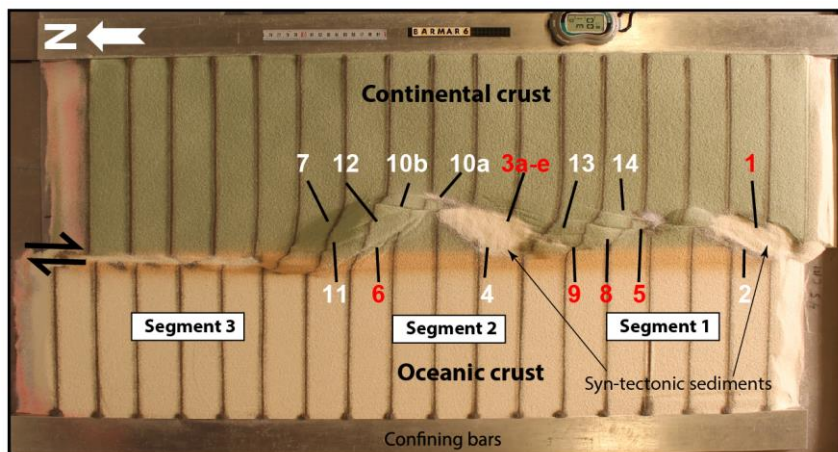


515  
 516 **Figure 3:** A) Schematic set-up of BarMar3-experiment as seen in map view. B) 517  
 518 Section through same experiment before deformation, indicating stratification 519  
 520 and thickness relations. C) Standard positions and orientation for sections cut in 521  
 522 all experiments in the BarMar-series. Yellow numbers are section numbers. Black 523  
 524 numbers indicate angle between the margins of the experiment (relative to N-S) 525  
 for each profile. D) Outline of silicone putty layer as applied in all experiments.

526 connected to an electronic engine, which pulled the sheet at constant velocity 527  
 528 during all three deformation stages. Displacement rates were therefore not 529  
 530 scaled. The modelling material was then placed on these sheets where the layers 531  
 532 on the stationary sheet represent the continental crust including the continent-  
 ocean transition (COT) whereas ~~the~~ those on the mobile sheet represents the  
 oceanic crust. The model layers ~~were~~ were confined by aluminum bars along the  
 long sides and sand along the short sides (Figure 3A). The ~~C~~ continental crust

533 tapers off towards the oceanic crust with a relatively constant gradient. A sand-  
 534 wedge with a constant dip angle determined by the difference in thickness  
 535 between the intact and the stretched crust, and that covered the width of the  
 536 silicon putty layer, was made to simulateing the ocean-continent-ocean transition  
 537 (Figure 3B). The taper angle was kept constant were included for in all models.

538  
 539 The pre-cut shape of the plate boundary includes major releasing bends  
 540 positioned so that they correspond to the geometry of the COB and the three main  
 541 structural segments of the Barents Shear Margin as follows. *Segment 1* of the  
 542 BarMar-experiments (Figure 4) contained several sub-segments with releasing  
 543 and restraining bends as well as segments of “neutral” (Wilcox et al., 1973; Mann  
 544 et al. 1983; Biddle & Christie-Blick, 1985b) or “pure” (Richard et al., 1991) strike-  
 545 slip. *Segment 2* had a basic crescent shape, thereby defining a releasing bend at its  
 546 southern margin in the position similar to that of the Vestbakken Volcanic  
 547 Province, that merged into a neutral shear-segment along the strike of, whereas a  
 548 restraining bend occupied the northern margin of the segment. *Segment 3* was a  
 549 straight basement segment, defining a zone of neutral shear and corresponds to  
 550 the strike-slip segment west of Svalbard (Figure 1).



551  
 552 **Figure 4:** Position of segments and major structural elements as referred to in the  
 553 text and subsequent figures (see particularly **Figures 5 and 6**). This example is  
 554 taken from the reference experiment BarMar6. All experiments BarMar6-9  
 555 followed the same pattern, and the same nomenclature was used in the  
 556 description of all experiments and provides the template for the definition of  
 557 structural elements in Figure 7.

558 The experiments included three stages of deformation with constant rates of  
559 movement of the mobile sheet at  $10 \text{ cmhr}^{-1}$  in all three stages. [The relative angles](#)  
560 [of plate movements in the experiments were taken from post--late Paleocene](#)  
561 [opening directions in the northeast Atlantic \(Gaina et al. 2009\)](#). Dextral shear was  
562 applied in the *first phase* in all experiments by pulling the lower plastic sheet by 5  
563 cm. In the *second phase* the left side of the experiment was extended by 3 cm  
564 orthogonally (BarMar6) or obliquely (325 degrees; BarMar 8 & 9) to the trend of  
565 the shear margin, whereas plate motion was reversed during the *third phase of*  
566 *deformation*, leading to inversion of earlier formed basins that had been  
567 developed in the strike-slip and extensional phases. Sedimentary basins that  
568 develop due to strike-slip (phase 1) or extension (phase 2) have been filled with  
569 layers of colored feldspar sand by sieving, [so that a smooth surface was obtained](#).  
570 These layers are primarily important for discriminating among deformation  
571 phases and thus act as marker horizons. Phase 3 was initiated by inverting the  
572 orthogonal (BarMar6) or oblique (BarMar 8 & 9) extension of Phase 2 as a proxy  
573 for ridge-push that likely was initiated when the mid-oceanic ridge was  
574 established in Miocene time in the North Atlantic (Moser et al., 2002; Gaina et al.,  
575 2009). Contraction generated by ridge-push has been inferred from the mid-  
576 Norwegian continental shelf (Våagnes et al., 1998; Pascal & Gabrielsen, 2001;  
577 Faleide et al., 2008; Gac et al., 2016) and seems still to prevail in the northern areas  
578 of Scandinavia (Pascal et al., 2005), although far-field compression generated by  
579 other processes have been suggested (e.g. Doré & Lundin, 1996).  
580  
581 Coloured layers of dry feldspar sand represent the brittle oceanic and continental  
582 crust. This material has proven suitable for simulating brittle deformation  
583 conditions (Willingshofer et al., 2005; Luth et al., 2010; Auzemery et al., 2021) and  
584 is characterized by a grain size of 100-200  $\mu\text{m}$ , a density of  $1300 \text{ kgm}^{-3}$ , a cohesion  
585 of  $\sim 16\text{-}45 \text{ Pa}$  and a peak friction coefficient of 0.67 (Willingshofer et al., 2018).  
586 Additionally, a 8 mm thick and of variable width corresponding to the ~~mapped~~  
587 [COT transition zone \(as mapped in reflection seismic data\)](#) of 'Rhodorsil Gomme  
588 GSIR' (Sokoutis, 1987) silicone putty mixed with fillers was used as a proxy for the  
589 thinned and weakened continental crust at the ~~ocean-continent-ocean~~ transition

590 **(Figure 1B and 3A,B)**. This Newtonian material ( $n=1.09$ ) has a density of 1330  
591  $\text{kgm}^{-3}$  and a viscosity of  $1.42 \times 10^4$  Pa.s.

592  
593 The experiments have been scaled following standard scaling procedures as  
594 described by Hubbert (1937), Ramberg (1967) or Weijermars and Schmeling  
595 (1986), assuming that inertia forces are negligible when modelling tectonic  
596 processes on geologic timescales (see Ramberg (1981) and Del Ventisette et al.  
597 (2007) for a discussion on this topic). The models were scaled so that 10 mm in  
598 the model approximates c. 10 km in nature yielding a length scale ratio of  $1.00 \times 10^6$ .  
599 As such, the model oceanic and continental crusts scale to 18 and 26 km in  
600 nature, respectively. A 26 km thick continental crust is a representative average  
601 for the crustal thickness east of the COT, ranging between 20 km in the SW Barents  
602 Sea and 30-32 km in the NW Barents Sea (Clark et al., 2012; Breivik et al. 2003). A  
603 thinning from 26 to 18 km across the COT is also realistic, however, the oceanic  
604 crust in the Norwegian-Greenland Sea is thinner than in the scaled model (Libak  
605 et al., 2012a,b), which, although slightly overestimating the most intensely  
606 thinned oceanic crust (10-12 km) is in full agreement with the estimated thickness  
607 of the thinned oceanward segment of the continental crust (30-20 km Breivik et  
608 al., 1998).

609  
610 The brittle crust, dry feldspar sand, deforms according to the Mohr-Coulomb  
611 fracture criterion (Horsfield, 1977; Mandl et al., 1977; McClay, 1990; Richard et  
612 al., 1991; Klinkmüller et al., 2016), whereas silicone putty promotes ductile  
613 deformation and folding. The geometry applied in the present experiments is  
614 accordingly well suited for the study of the COB/COT in the Barents Shear Margin  
615 (Breivik et al., 1998).

616  
617 When complete, the experiments were covered with a thin layer of sand further to  
618 stabilize the surface topography before the models were saturated with water and  
619 cross-sections that were oriented transverse to the velocity discontinuity were cut  
620 in a fan-shaped pattern (**Figure 3C**). All experiments have been monitored with a  
621 digital camera providing top-view images at regular time intervals of one minute.  
622

623 All experiments performed were oriented in a N-S-coordinate framework to  
624 facilitate comparison with the western Barents Sea area and had a three-stage  
625 deformation sequence (dextral shear – opening – closure). All descriptions and  
626 figures relate to this orientation. It was noted that all experiments reproduced  
627 comparable basic geometries and structural types, demonstrating robustness  
628 against variations in contrasting strength of the “~~ocean-continent-ocean~~”-  
629 transition zone, which included ~~by~~ a zone of silicone putty with variable width  
630 below ~~an~~ eastward thickening sand-wedge (**Figure 3B**) and changing  
631 displacement velocities.

632

### 633 **Modelling Results**

634

635 A series of ~~totally~~ nine experiments (BarMar1-9) with the set-up described above  
636 was performed. Experiments BarMar1-5 were used to calibrate and optimize  
637 geometrical outline, deformation rate, and angles of relative plate movements and  
638 are not shown here. The optimized geometries and experimental conditions ~~were~~  
639 utilized for experiments BarMar6-9, of which BarMar6 and 8 (and some examples  
640 from BarMar9) ~~and~~ are illustrated here, yielded similar results in that all crucial  
641 structural elements (faults and folds) were reproduced in all experiments as  
642 described in the text ~~and are~~ shown in **Figure 4.** It is emphasized that the  
643 extensional basins affiliated with the extension phase (phase 2) became wider in  
644 the orthogonal (BarMar6) as compared to oblique extension experiments (BarMar  
645 8) (**Figures 5 and 6**). Furthermore, the fold systems generated in the experiments  
646 that utilized oblique contraction of  $325/145^{\circ}$  (BarMar8-9) produced more  
647 extensive systems of non-cylindrical folds with continuous, but more curved fold  
648 traces as compared ~~to~~ experiments with orthogonal extension/contraction  
649 (BarMar6). The fold axes generally rotated to become parallel to the (extensional)  
650 master faults delineating the pull-apart basins generated in deformation stage 1  
651 in experiments with an oblique opening/closing angle.

652 Examples of the sequential development is displayed in **Figures 5 and 6**) and  
653 summarized in **Figure 7**.

654

655 Elongate positive structural elements with fold-like morphology as seen on the  
656 surface were detected during the various stages of the present experiments. The  
657 true nature of those were not easily determined until the experiments were  
658 terminated and transects could be examined. Such structures included buried  
659 push-ups (*sensu* Dooley & Schreurs, 2012), antiformal stacks, back-thrusts,  
660 positive flower structures, fold trains, and simple anticlines. For convenience, we  
661 use the non-genetic term “positive structural elements” termed *PSE-m-n* for such  
662 structure types as seen in the experiments in the following description.  
663 In the following the deformation in each segment is characterized for the three  
664 deformation phases ([Table 1](#)).

Formatted: Font: Bold

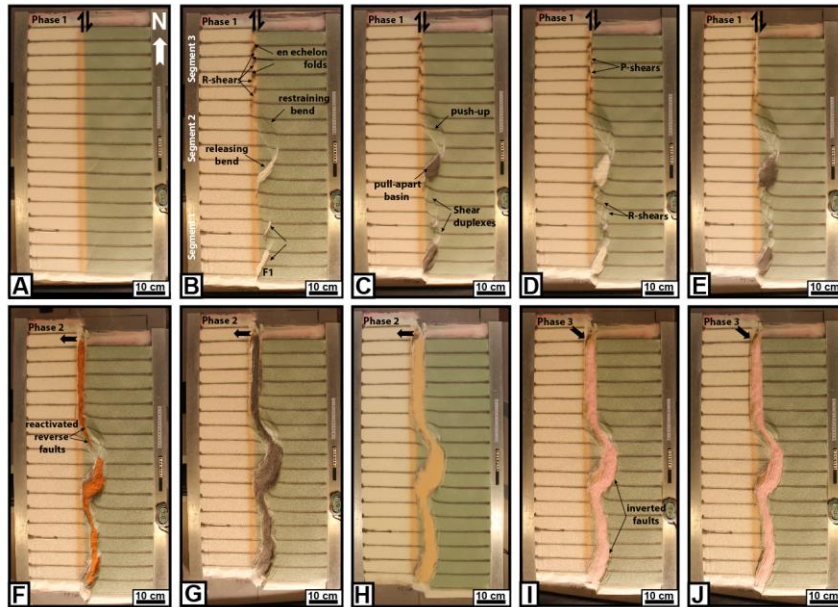
#### 666 **Deformation phase 1: Dextral shear stage**

667  
668 *Segment 1:* Differences in the geometry of the pre-cut fault trace between  
669 segments 1, 2 and 3 became evident after the very initial deformation stage.  
670 Particularly in segments 1 and 3 an array of oblique *en échelon* folds in between  
671 Riedel shear structures (*PSE-1-structures*) oriented c. 1345° (NW-SE) to the  
672 regional VD rotating ~~towards into a NNW-SSE-orientation~~ by continued shear  
673 (**Figure 8**; see also Wilcox et al., 1973; Ordonne & Vialon, 1983; Richard et al.,  
674 1991; Dooley & Schreurs, 2012). These were simple, harmonic folds with upright  
675 axial planes and fold axial traces extending a few cm beyond the surface shear-  
676 zone described above. They had amplitudes on the scale of a few millimeters and  
677 wavelengths on scale of 5 cm. The *PSE-1-structures* interfered with or were  
678 dismembered by younger ~~developing~~ structures (*Y-shears and PSE-2-structures*;  
679 [see below](#)), ~~also~~ causing northerly rotation of individual intra-fault zone lamellae  
680 (remnant *PSE-1-structures*; ~~(Figure 8)~~). Structures similar to *PSE-1-fold arrays*  
681 are known from almost all strike-slip experiments reported and described in the  
682 literature from the early works of (e.g. Cloos, 1928; Riedel, 1929. See Dooley &  
683 Schreurs, 2012 for summary) and are therefore not given further attention here.

684  
685 By 0.25 cm of horizontal displacement in segment 1, which included ~~two~~ releasing  
686 and restraining bends ~~separated by in combination with a central strands~~ of  
687 neutral shear, a slightly curvilinear surface trace of a NE-SW-striking, top-NW

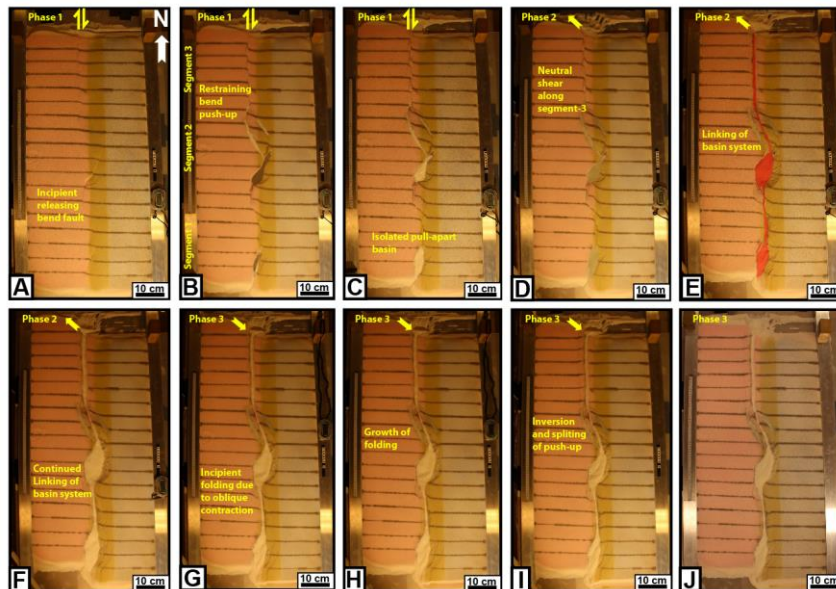
688 normal faults in the southernmost part of segment 1 developed. This co-existed  
689 with the PSE-1-structures and was immediately paralleled by a normal fault with  
690 opposite throw (fault 2, **Figure 4**) so that the two faults constrained a crescent- or  
691 spindle-shaped incipient extensional shear duplex (**Figures 5B and 6B**; see also  
692 Mann et al., 1983; Christie-Blick & Biddle, 1985; Mann 2007; Dooley & Schreurs,  
693 2012).

694  
695 A system of *en échelon* faults separate N-S to NNE-SSE- striking normal and shear  
696 fault segments became visible in segment 1 after ca. 1 cm of shear (**Figure 5C,D**).  
697 These faults did not have the orientations as expected for R ([Riedel](#)) - and R' ([anti-](#)  
698 [Riedel](#))- shears ([that would be oriented with angles of approximately 15 and 75°](#)  
699 [from the master fault trace](#)), but became progressively linked by along-strike  
700 growth and the development of new faults and fault segments. They thereby  
701 acquired the characteristics of Y-shears ([oriented sub-parallel to the master fault](#)  
702 [trace](#)), dissecting the PSE-1-structures. By 2.4 cm of shear, segment 1 had become  
703 one unified fault array (**Figures 5D and 6D**), delineating a system of incipient  
704 push-ups or positive flower structures (*PSE-2-structures*; **Figures 8 and Figure**  
705 **10, sections B1 and B3**, see also; Riedel, 1929; Wilcox et al., 1973; Odonne &  
706 Vialon, 1983; Dauteuil & Mart, 1995; Dooley & Schreurs, 2012).



707  
 708 **Figure 5:** Sequential development of experiment BarMar6 by 0.5, 2.4, 3.5, 4.0 and  
 710 5.0 cm of dextral shear (Steps A-E), orthogonal extension (steps F-H) and  
 711 oblique contraction (steps I-J). The master fault strands are numbered in **Figure 4**, and  
 712 the sequential development for each structural family is shown in **Figure 7**.

713  
 714 The PSE-2-structures had amplitudes of 1 - 2 cm and wavelengths of 3 - 5 cm as  
 715 measured on the surface with fault surfaces that steepened down-section, the  
 716 deepest parts of the structures having cores of sand-layers deformed by open to  
 717 tight folds. The folds had upright or slightly inclined axial planes, dipping up to  
 718 55°, mainly to the east. The structures also affected the shallowest layers down to  
 719 1-2 cm in the sequence, but the shallowest sequences were developed at a later  
 720 stage of deformation and were characterized by simple gentle to open anticlines.  
 721 These structures were constrained to a zone of deformation directly above the  
 722 trace of the basement fault, similar to that commonly seen along shear zones (e.g.  
 723 Tchalenko, 1971; Crowell, 1974 a,b; Dooley & Schreurs, 2012). This zone was 3-4  
 724 cm wide and remained stable throughout deformation stage 1 and -was restricted



725

726 **Figure 6:** Sequential development of experiment BarMar8 by 1.0, 3.5 and 5.0 cm  
 727 of dextral shear (Steps A-C), oblique extension (steps D-F) and oblique contraction  
 728 (steps G-I). Step J represents the final model after end of contraction. The master  
 729 fault strands are numbered in **Figure 3**, and the sequential development for each  
 730 structural family is shown in **Figure 7**. Phases 2 and 3 involved oblique ( $325^{\circ}$ )  
 731 extension and contraction in this experiment.

732

733 to the close vicinity of the basement shear fault itself as also described from one-  
 734 stage shear faults in Riedel box-type experiments (e.g. Tchalenko, 1970; Naylor et  
 735 al., 1986; Richard et al., 1991; Casas et al., 2001; Dauteuil & Mart, 1998; Dooley &  
 736 Schreurs, 2012) and from nature as well (e.g. Wilcox et al., 1973; Harding, 1974;  
 737 Harding & Lowell, 1979; Sylvester, 1988; Woodcock & Schubert, 1994; Mann,  
 738 2007).

739

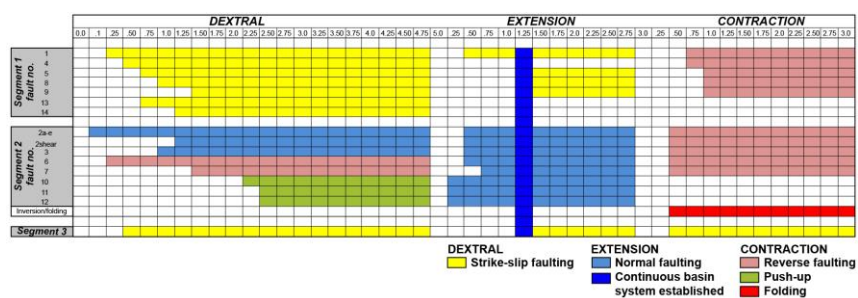
740 A horse-tail-like fault array developed by ca. 3 cm of shear at the transitions  
 741 between segments 1 and 2 (see also Cunningham & Mann, 2007; Dooley &  
 742 Schreurs, 2012, their Figure 44) (**Figures 5B-D and 6B-D**).

743

744 The structuring in *Segment 2*; was ruled by the crescent-shaped basement fault  
 745 (VD) that generated a releasing bend along its southern and a restraining bend  
 746 along its northern border (**Figure 11**). The first fault of fault array 3a-e in the

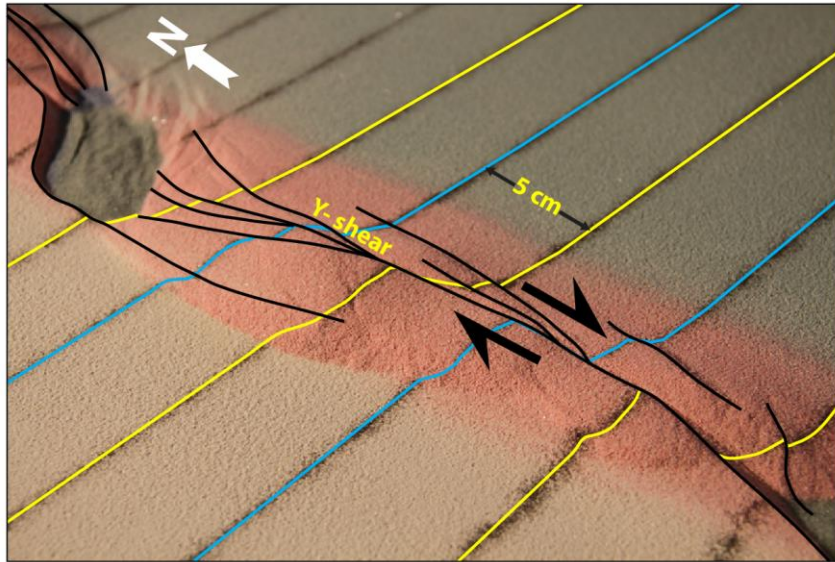
747 southern part of Segment 2 was activated after c. 0.15 cm of bulk horizontal  
 748 displacement (**Figure 7**). It was situated directly above the southernmost precut  
 749 releasing bend, defining the margin of crescent-shaped incipient extensional  
 750 strike-slip duplexes (in the context of Woodcock & Fischer, 1986, Woodcock &  
 751 Schubert, 1994 and Twiss & Moores, 2007, p. 140-141). The developing basin got  
 752 a spindle-shaped structure and developed into a basin with a lazy-S-shape  
 753 (Cunningham & Mann, 2007; Mann, 2007). The basin widened towards the east by  
 754 stepwise footwall collapse, generating sequentially rotating crescent-shaped  
 755 extensional fault blocks that became trapped as extensional horses in the footwall  
 756 of the releasing bend (**Figure 11**). In the areas of the most pronounced extension,  
 757 the crestal part of the rotational fault blocks became elevated above the basin  
 758 floor, generating ridges that influenced the basin floor topography and hence, the  
 759 sedimentation. By continued rotation of the fault blocks and simultaneous sieving  
 760 of sand the crests of the blocks became sequentially uplifted, sieving of sand layer  
 761 on generating the top of these structures, forced folds (Hamblin, 1965; Stearns,  
 762 1978; Groshong, 1989; Khalil & McClay, 2016) were generated (**Figure 10A**). In  
 763 the analysis we used the term *PSE-3-structures* for these features. Simultaneously,  
 764 an expanding sand-sequence became trapped in the footwalls of the master faults,  
 765 defining typical growth-fault geometries.

767 By a shear displacement of 0.55 cm additional curved splay faults were initiated  
 768 from the northern tip of the master fault of fault 3f; (**Figure 7**), delineating the  
 769 northern margin of a rhombohedral pull-apart-basin (Mann et al., 1983; Mann,



770  
 771 **Figure 7:** Summary of sequential activity in each master structural element  
 772 (**Figure 4**) in Experiment BarMar6 (**Figure 5**). Type and amount of displacement  
 773 is shown in two upper horizontal rows. The vertical blue bar indicates the stage at

774 which full along-strike communication became established between marginal  
775 basins. Color code (see in-set) indicates type of displacement at any stage.  
776



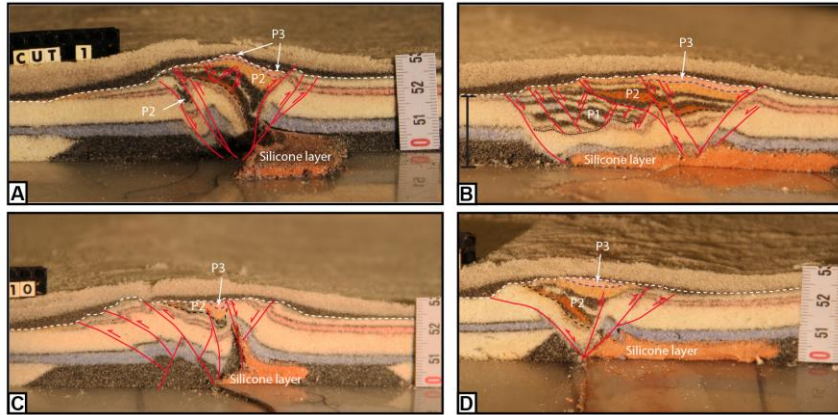
777  
778 **Figure 8:** PSE-1 anticline-syncline pairs in segment 1 experiment BarMar6 in an  
779 oblique view. PSE-1 folds were constrained to the very fault zone and the fold axes  
780 (blue lines) and extended only 3-4 cm beyond the fault zone. PSE-2 structures  
781 (incipient shear-duplex and positive flower structures; yellow lines) were  
782 delineated by shear faults and completely cannibalized PSE-1 structures by  
783 continued shear. Yellow and blue lines show the rotation of the fold axial trace  
784 caused by dextral shearing of c. 1,5 cm. 25mm of dextral shear. By a displacement  
785 of 35mm the remains of the PSE-1 structure was completely obliterated. The  
786 distance between the markers (dark lines) is 5cm. Yellow arrow marks north-  
787 direction. White arrows indicate shear direction.  
788

789 2007; Christie-Blick & Biddle, 1985) and with a geometry that was  
790 indistinguishable from pull-apart basins or rhomb grabens affiliated with  
791 unbridged *en échelon* fault arrays (Crowell, 1974 a,b; Aydin & Nur, 1993).  
792 Although sand was filled into the subsiding basins to minimize the graben relief  
793 and to prevent gravitational collapse, the sub-basins that were initiated in the  
794 shear-stage were affected by internal cross-faults, and the initial basin units  
795 remained the deepest so that the buried internal basin topography maintained a  
796 high relief with several apparent depo-centers separated by intra-basinal  
797 platforms.

798  
799 Systems of linked shear faults and PSE-structures became established in the  
800 central part with neutral shear that separate the releasing and restraining bends  
801 and development similarly to that seen for segment 3 (see below). ~~but~~ However,  
802 these structures were soon destroyed by the combined development of the  
803 northern and southern tips of the extensional and contractional shear duplexes  
804 (**Figure 10**).

805  
806 The first structure to develop in the regime of the restraining bend (segment 2;  
807 was a top-to-the-southwest (antithetic) thrust fault at an angle of  $145^{\circ}$  with the  
808 regional trend of the basement border as defined by segments 1 and 3 (Fault 6). It  
809 became visible by 0.5 cm of displacement. The northern part of segment 2 became,  
810 however, dominated by a synthetic contractional top-to-the-northeast fault that  
811 was initiated by 0.85 cm of shear (Fault 7; **Figures 5 and 6**). Thus, faults 6 and 7  
812 delineated a growing half-crescent-shaped 5-7-cm wide push-up structure (Aydin  
813 & Nur, 1982; Mann et al., 1983) south of the restraining bend (**Figure 9**; PSE-4-  
814 structures). By continued shear these structures got the character of an antiformal  
815 stack.

816  
817 *Segment 3* defined a straight strand of neutral shear. Its development in the  
818 BarMar-experiments followed strictly that known from numerous published  
819 experiments (e.g. Tchalenko, 1970; Wilcox et al., 1973; Harding, 1974; Harding &  
820 Lowell, 1979; Naylor et al., 1986; Sylvester, 1988; Richard et al., 1991; Woodcock  
821 & Schubert, 1994; Dauteuil & Mart, 1998; Mann, 2007; Casas et al., 2001; Dooley

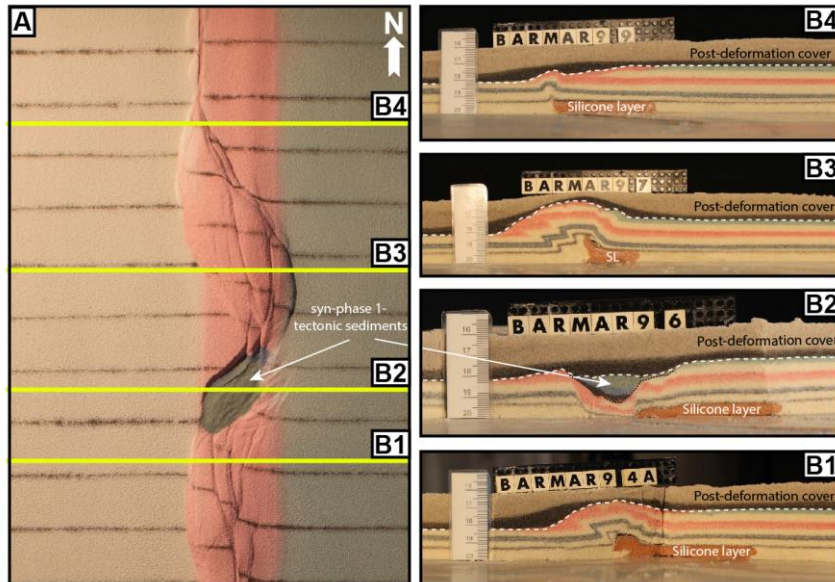


822

823 **Figure 9:** Cross-sections through PSE-2-related structures. **A)** Folded core of  
 824 incipient push-up/positive flower structure in segment 1, experiment BarMar6.  
 825 The fold structure is completely enveloped of shear faults that have a twisted  
 826 along-strike geometry. Note that the eastern margin of the structure developed  
 827 into a negative structure at a late stage in the development (filled by black-pink  
 828 sand sequence) and that the silicone putty sequence (basal pink sequence) was  
 829 entirely isolated in the footwall. **B)** Similar structure in experiment BarMar8. The  
 830 weak silicone putty layer here bridged the high-strain zone and focused folding  
 831 that propagated into the sand layers (blue). The folds in upper (pink layers) were  
 832 associated with the contraction stage, because they contributed to a surface relief  
 833 filled in by red-black-sand sequence that was sieved into the margin during the  
 834 contraction stage. **C)** Contraction associated with “crocodile structure” in the  
 835 footwall of the main fault in segment 1, experiment BarMar8. Note disharmonic  
 836 folding with contrasting fold geometries in hanging wall and footwall and at  
 837 different stratigraphic levels in the footwall, indicating shifting stress situation in  
 838 time and space in the experiment. **D)** Transitional fault strand between to more  
 839 strongly sheared fault segments (experiment BarMar9).

840

841 & Schreurs, 2012). A train of Riedel-shears, occupying the full length of the  
 842 segment, appeared simultaneously on the surface after a shear displacement of  
 843 0.5 cm, occupying a restricted zone with a width of 2-3 cm. The Riedel-shears  
 844 dominated the continued structural development of Segment 3. Riedel'-shears  
 845 were absent throughout the experiments, as should be expected for a sand-  
 846 dominated sequence (Dooley & Schreurs, 2012). P-shears developed by continued  
 847 shear, creating linked rhombic structures delineated by the Riedel- and P-shears  
 848 generating positive structural elements with NW-SE- and NNE-SSE-striking axes  
 849 (see also Morgenstern & Tchalenko, 1967), soon coalescing to form Y-shears.  
 850 Transverse sections document that these structures were cored by push-up



851

852 **Figure 10: A)** contrasting structural styles along the master fault system in  
 853 segment 2 in map view and **(B)** cross sections of experiment BarMar9. SL denotes  
 854 silicone layer, the stippled line the boundary between pre- and syn-deformation  
 855 layers and the white dashed line the boundary with the post-deformation layers.  
 856

857 anticlines, positive half-flower structures. The segments with neutral shear would  
 858 generate and full-fledged positive flower structures in the advanced stages of  
 859 shear (PSE-4-structures) (Figures 5 and 6. See also Figure 10). These were  
 860 accompanied by the development of *en échelon* folds and flower structures as  
 861 commonly reported from strike-slip faults in nature and in experiments. The  
 862 width of the zone above the basal fault remained almost constant throughout the  
 863 experiments, but was somewhat wider in experiments with thicker basal silicone  
 864 polymer layers, similar to that commonly described from comparable  
 865 experiments (e.g. Richard et al., 1991).  
 866

### 867 **Deformation Phase 2: Extension**

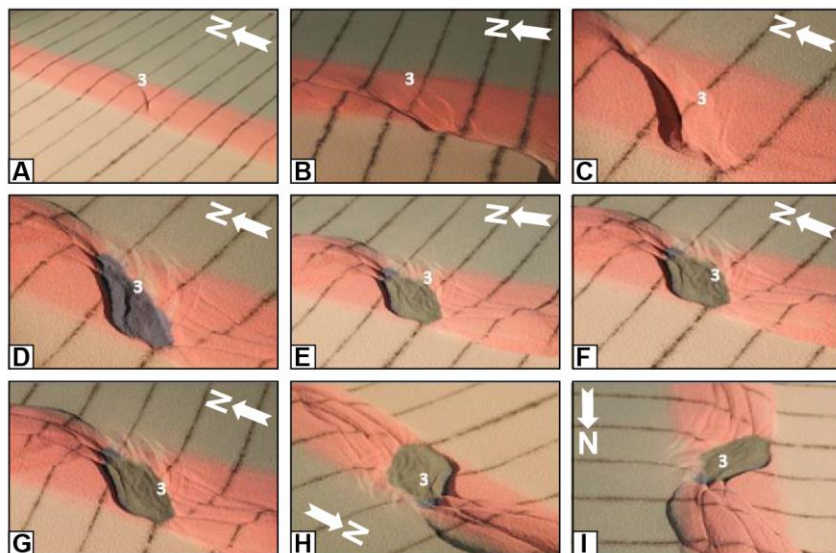
868

869 The ~~late-Cretaceous~~-Palaeogene dextral shear was followed by pure extension  
 870 accompanying the opening along the Barents Shear Margin in the Oligocene. Our

Formatted: Font: Italic

Formatted: Font: Italic

871 experiments utilized focused on the effects of oblique extension, acknowledging  
872 that plate tectonic



873  
874 **Figure 11:** Nine stages in the development of the extensional shear duplex system  
875 above the releasing bend in experiment BarMar9. The master faults that  
876 developed at an incipient stage (e.g., Fault 3 that constrained the eastern margin  
877 of the extensional shear duplex) remained stable and continued to be active  
878 throughout the experiment (Figure 7), but became overstepped by faults in its  
879 footwall that became the basin contraction faults at the later stages H and I. Note  
880 that the developing basement was stabilized by infilling of gray sand during this  
881 part of the experiment. Note that Fault 3 remained active and broke through the  
882 basin infill also after the basin infill overstepped the original basin margin. The  
883 distance between the markers (dark lines) is 5cm. Yellow arrow marks north-  
884 direction. Note that figure I has a different orientation.  
885

886 reconstructions of the North Atlantic suggest an extension angle of  $325^\circ$  as the  
887 most likely (Gaina et al., 2009).

888  
889 All strike-slip basins widened in the extensional stage, and most extensively so for  
890 the experiments with orthogonal extension. The widening of the basin enhanced  
891 the topography already generated in the shear-stage in the extensional strike-slip  
892 duplex in segment 2 (PSE-33-structures). In the earliest extensional-stage the  
893 strike-slip basin in segment 2 dominated the basin configuration, but by continued  
894 extension the linear segments and the minor pull-apart basins in segments 1 and

895 2 started to open and became interlinked, subsequently generating a linked basin  
896 system that paralleled the entire shear margin (**Figures 5F-G, 6F-G**).

897

898 The ~~orthogonal~~ extension-phase following dextral strike-slip reactivated and very  
899 quickly linked several of the master faults that were established in deformation  
900 phase 1 (**Figures 5A and 6A**) already by an extension of 0,25 – 0,50 cm. This  
901 included the southern fault margin, the push-up and the splay faults defining a  
902 crestral collapse graben of the push-up (Faults 6, 11 and 12; **Figure 4**). All three  
903 segments were reactivated in extension by c. 1.25 cm of orthogonal stretching  
904 (**Figure 7**). During the first cm of extension each basin remained an isolated unit,  
905 but after 1 cm of extension all basins became linked, thus forming one unified  
906 elongate extensional basin (marked by the vertical dark blue line in **Figure 7**) and  
907 mainly following the PDZ as it was cut in the basal templates. Among the faults  
908 that were inactive and remained so throughout the extension phase were the  
909 antithetic contractional fault delineating the push-ups in segment 2 towards the  
910 south (Fault 6; **Figure 4**). The Y-shear in Segment 3 was reactivated as a straight,  
911 continuous extensional fault in Stage 2. Total extension in Phase 3 was 5 cm.

912

### 913 **Deformation Phase 3: ~~e~~Contraction**

914

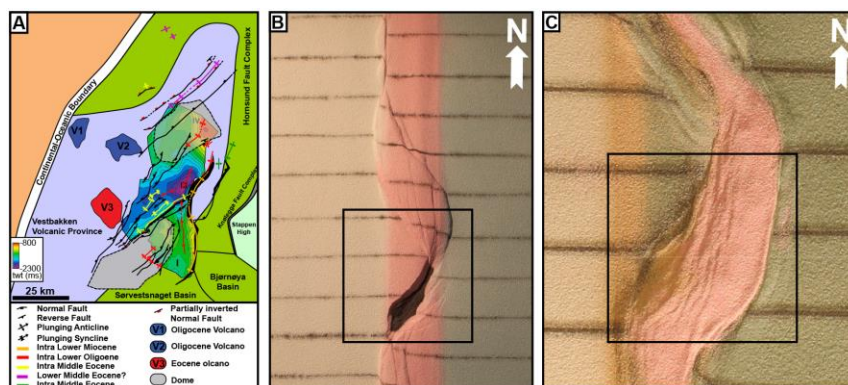
915 In our experiments the extension stage was followed by orthogonal or oblique  
916 contraction (parallel to the direction of extension as applied for each experiment).  
917 The experiments were terminated before the full closure of the basin system, in  
918 accordance with ~~i.e.~~ the extension vector > contraction vector as in the North  
919 Atlantic (see Vågnes et al., 1998; Pascal & Gabrielsen 2001; Gaina et al. 2009). A  
920 part of the early-stage contraction was accommodated along new faults. It was  
921 more common, however, that faults that had been generated in the strike-slip and  
922 extensional stages became reactivated and rotated, and the development of  
923 isolated folds, which were commonly associated with inverted fault traces,  
924 generating snake-head- or harpoon-type structures (Cooper et al.,  
925 1989; Coward, 1994; Allmendinger, 1998; Yameda & McClay, 2004; Pace &  
926 Calamitra, 2014); PSE-5-structures). This was particularly the case for the master  
927 faults, as seen by continued or accelerated subsidence. The dominant structures

Formatted: Font: 12 pt

Formatted: Font: 12 pt

Formatted: Font: Italic

928 affiliated with the contractional stage was still new folds with traces oriented  
 929 orthogonal to the shortening direction and sub-parallel to the preexisting master  
 930 fault systems that defined the margin and basin margins (**Figure 12**). Also,



931  
 932 **Figure 12:** PSE-5 and PSE-6 folds generated during phase 3-inversion, experiment  
 933 BarMar8. Note that fold axes mainly parallel the basin rims, but that they deviate  
 934 from that in the central parts of the basins in some cases. Note that the folds are  
 935 best developed in segment 2, which accumulated extension in the combined shear  
 936 and extension stages.

938 some deep fold sets that had been generated during the strike-slip phase and seen  
 939 as domal surface features became reactivated, causing renewed growth of surface  
 940 structures (see **Figure 10** and explanation in figure caption). These folds were  
 941 generally up-right cylindrical buckle folds in the initial contractional stage and  
 942 with very large trace length: amplitude-ratio (*SPE-65-structures*). Some intra-  
 943 basin~~a~~ folds, however, defined fold arrays that diagonally crossed the basins.  
 944 Particularly the folds situated along the basin margins developed into fault  
 945 propagation-folds above low-angle thrust planes. Such faults aligning the western  
 946 basin margins could have an antithetic attitude relative to the direction of  
 947 contraction.

948  
 949 During the contractional phase the margin-parallel, linked basin system started  
 950 immediately to narrow and several fault strands became inverted. The basin-  
 951 closure was a continuous process until the end of the experiment by 3 cm of  
 952 contraction. The contraction was initiated as a proxy for an ESE-directed ridge-  
 953 push stage. The first effect of this deformation stage was heralded by uplift of the

954 margin of the established shear zone that ~~that~~ had developed into a rift during  
955 deformation stage 2. This was followed by the reactivation and inversion of some  
956 master faults (e.g., fault a2; ~~e.g. Figure 4~~) and thereafter by the development of a  
957 new set of low-angle top-to-the-ESE contractional faults. These faults displayed a  
958 sequential development, (~~fault family 1; Figure 4~~) and were associated with  
959 folding of the strata in the rift structure, probably reflecting foreland-directed in-  
960 sequence thrusting ([SPSE-5 and PSE-6 fold populations](#)).

961  
962

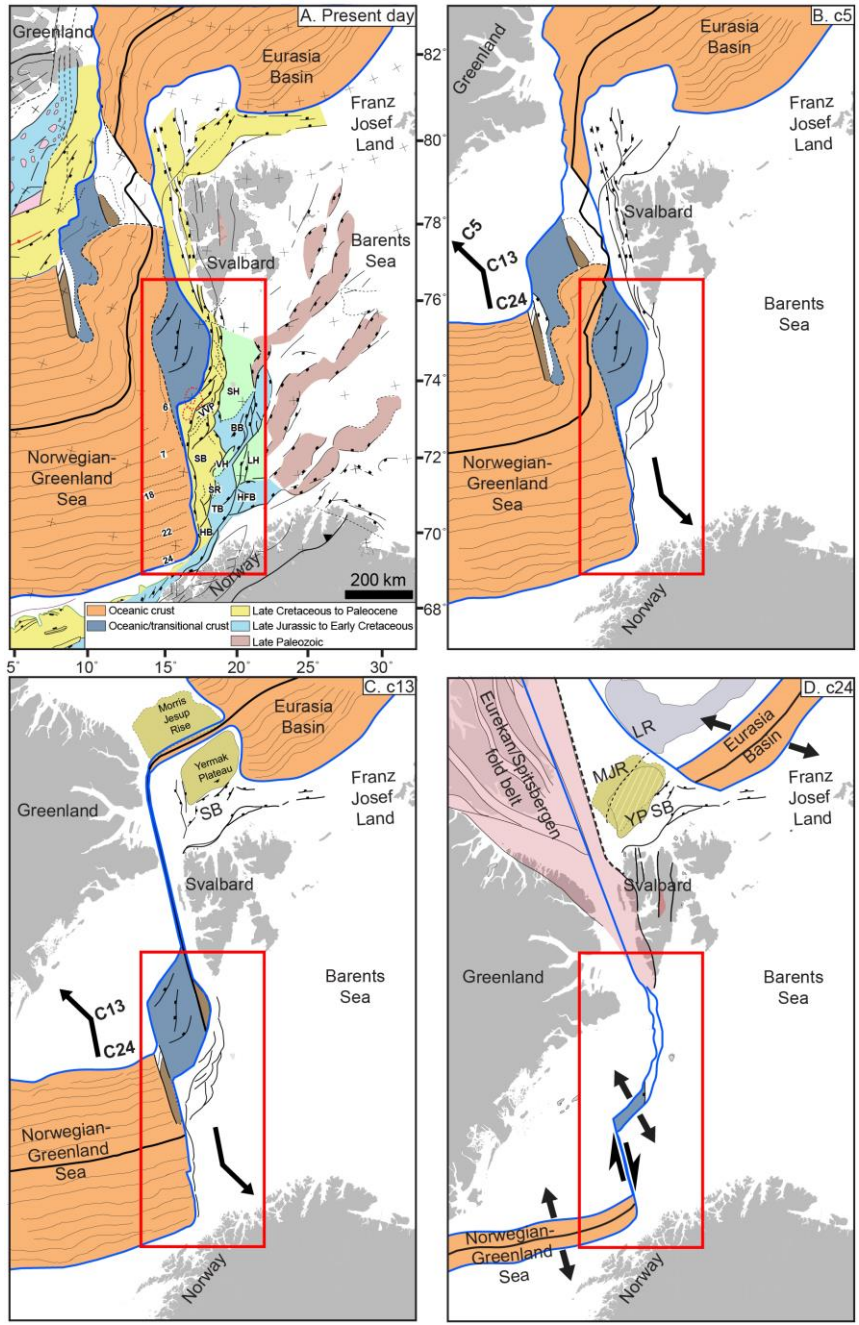
## 963 Discussion

964  
965 The break-up and subsequent opening of the Norwegian-Greenland Sea was a  
966 multi-stage event (**Figure 13**) that imposed shifting stress [configurations](#)  
967 ~~overprinting relation on~~ the already geometrically complex Barents Shear Margin.  
968 ~~The incipient stages occurred in the late Cretaceous — early Palaeocene (e.g.~~  
969 ~~Eldholm et al 1987; Vågnes, 1997; Myhre & Eldholm, 1988; Gabrielsen et al., 1990;~~  
970 ~~Gudlaugsson & Faleide, 1994; Knutsen & Larsen, 1997; Ryseth et al., 2003; Faleide~~  
971 ~~et al., 1993; 2008; Reemst et al., 1994; Bergh & Grogan, 2003; Kristensen et al.,~~  
972 ~~2017), and the development included extensive volcanism (Eldholm et al., 1989;~~  
973 ~~Saunders et al., 1997; Planke et al., 1999; Ganerød et al., 2010; Horni et al., 2017).~~  
974 ~~Opening accelerated and was accompanied by extensive marine sedimentation in~~  
975 ~~the Eocene and changed into a passive margin setting from the earliest Oligocene.~~  
976 ~~The spreading stage was likely associated with ridge push (e.g. Doré & Lundin,~~  
977 ~~1996; Vågnes et al., 1998; Pascal & Gabrielsen, 2001), plate reorganization~~  
978 ~~(Talwani & Eldholm, 1977, Gaina et al., 2009) or other far field stresses (Doré &~~  
979 ~~Lundin, 1996; Lundin & Doré, 1997; Doré et al., 1999; Lundin et al., 2013). Faults,~~  
980 ~~and fold arrays associated with shear and tectonic inversion as well as elements~~  
981 ~~of subsidence/elevation are obviously prominent for the deduction of the~~  
982 ~~structural history in such systems (e.g. Cloos, 1928, 1955; Riedel, 1929; Campbell,~~  
983 ~~1953; Tchalenko, 1970; Wilcox et al., 1973; Dauteuil & Mart, 1998; Odonne &~~  
984 ~~Vialon, 1983; Richard et al., 1991; Richard & Kranz, 1991; Dooley & McClay, 1997;~~  
985 ~~Basile & Brun, 1999; Mitra & Paul, 2011; Dooley & Schreurs, 2012; Kristensen et~~  
986 ~~al., 2017). Therefore, scaled experiments were designed to illuminate the~~

987 ~~structural developmentse-complexities~~ of the Barents Shear Margin. The  
988 experiments utilized three main segments that correspond to the Senja Fracture  
989 Zone (segment 1), the Vestbakken Volcanic Province (segment 2) and the  
990 Hornsund Fault Zone (segment 3). A series of structural families developed during  
991 the experiments, most of which correspond to structural elements found along the  
992 Barents Shear Margin.

993  
994 Segment 1 in the experiments (which correponds to the Senja ~~Shear~~  
995 ~~MarginFracture-Zone~~) was dominated by neutral dextral shear, although  
996 subordinate jogs in the (pre-cut) fault provided minor sub-segments with mainly  
997 releasing and subordinate restraining bends. PSE-1-folds, that developed at an  
998 incipient stage were immediately paralleled by two sets of normal faults with  
999 opposite throw in the releasing bend areas (e.g., fault 2; **Figure 4**). ~~so that T~~the  
1000 two faults ~~definedconstrained~~ a crescent- or spindle-shaped incipient extensional  
1001 shear duplex ~~became evident~~ (**Figures 5B and 6B**; see also Mann et al., 1983;  
1002 Christie-Blick & Biddle, 1985; Mann, 2007; Dooley & Schreurs, 2012). The most  
1003 prominent of these structures corresponds to the position of the Sørvestsnaget  
1004 Basin (**Figure 1B**).

1005  
1006 Counterparts to PSE-1 and PSE-2 structural populations observed in the  
1007 experiments were not identified with certainty in the seismic data along the  
1008 Barents Shear Margin, although some isolated, local anticlinal features could be  
1009 dismembered remnants of such. The PSE-1 and PSE-2 structures generally  
1010 belongs to the structural populations that were developed at the earliest stages of  
1011 the experiments. Furthermore, these structure types were confined to the area  
1012 just



1013  
 1014 **Figure 13;** Main stages in opening of the North Atlantic. A) Present day, B) chron  
 1015 5 (10 Ma in the late Miocene), C) chron 13 (33 Ma in the earliest Oligocene), D)  
 1016 chron 24 (53 Ma in the early Eocene).

1017 above the basal master fault (VD) and its immediate vicinity (see also experiments  
1018 in series “e” and “f” of Mitra & Paul, 2011). Because of their constriction to the near  
1019 vicinity of the master fault, we speculate that sStructures generated at an early  
1020 stage ~~of shear, in a developing, multistage systems that involve shear, extension~~  
1021 and contraction are vulnerable to soon became overprinted and canabalisation  
1022 ~~zed~~-by younger structures with axes striking parallel to the main shear fault (Y-  
1023 shears; SPE-2-structures). ~~The strike-slip stage of the experiments is comparable~~  
1024 ~~to the experiments in series “e” and “f” of Mitra & Paul (2011). It is particularly~~  
1025 ~~emphasized that SPE-1 and SPE-2-structures were confined to the area just above~~  
1026 ~~the basal master fault (VD) and its immediate vicinity. Although careful search for~~  
1027 ~~positive early (PSE-1) in the reflection seismic data was conducted, no remains of~~  
1028 ~~such structures were detected.~~We therefore conclude that the majority of these  
1029 structure populations were destroyed during the later stages of shear and during  
1030 the subsequent stages of extension and contraction.

1031  
1032 During the oblique extension stage segment 1 of experiments BarMar7-9 ~~twere~~  
1033 ~~characterized by oblique opening.~~ The basin subsidence was focused in the minor  
1034 pull-apart basins, which soon became linked along the regional N-S-striking basin  
1035 axis. Remains of several such basin centers, of which the Sørvestsnaget Basin  
1036 (Knutsen & Larsen, 1997; Kristeianen et al., 2017) is the largest, are preserved  
1037 and found in seismic data (**Figure 1b**). During the experiments a continuous basin  
1038 system was developed in the hangingwall side of the master fault, but it is not  
1039 likely that opening occurred prior to the extension of the margin underlain by  
1040 continental crust reached a stage where the separate basin units ~~such a superior~~  
1041 ~~basin system ever existed paralleling along~~ the Barents Shear Margin became  
1042 linked.

1043  
1044 In the subsequent inversion stage, fold trains with axial traces parallel (PSE-5-  
1045 folds) to the basin axis and the master faults characterized segment 1. Remnants  
1046 of such folds are locally preserved in the thickest sedimentary sequences affiliated  
1047 with the Senja Shear Margin.

1048

1049 Segment 2, which was underlain by a crescent-shaped discontinuity corresponds  
1050 to the Vestbakken Volcanic Province and the southern extension of the Knølegga  
1051 Fault Complex that is a branch of the southern part of the Hornsund Fault Zone  
1052 (**Figures 1b and 4**). The part of the Vestbakken Volcanic Province that was the  
1053 subject of structural analysis by Giennenas (2018) corresponds to the southern  
1054 part of segment 2 in the present experiments. It is dominated by interfering NNW-  
1055 SSE- and NE-SW striking fold- and fault systems in the central part of the basin,  
1056 whereas N-S-structures are more common along its eastern margin (**Figure 12A**)  
1057 (Jebsen & Faleide, 1998; Giennenas, 2018).

1058  
1059 Intra-basinal platforms and complex internal configurations seen in the BarMar-  
1060 experiments are common in strike-slip basins (e.g. Dooley & McClay, 1997;  
1061 Dooley & Schreurs, 2012) and are consistent with the structural configuration  
1062 with intra-basinal depo-centers within the Vestbakken Volcanic Province and  
1063 also in the Sørvestsnaget Basin (Knutson & Larsen, 1997; Jebsen & Faleide, 1998;  
1064 **Figure 13**).

1065 The positive structural elements that prevail in *segment 3* are similar to PSE-1 and  
1066 belong to the PSE-2-structure populations, described for segment 1. The  
1067 structures affiliated with segment 3 in the BarMar-experiments are similar  
1068 correspond well to those seen in the reflection seismic sections along parts of  
1069 the Spitsbergen and the Senja shear margins (Myhre, et al., 1982; Faleide et al.,  
1070 1993). Thus, the structuring in the segment 3 in the BarMar-experiments display  
1071 a configuration typical for followed strictly the pattern well established for  
1072 neutral shear in that an array of NW-SE striking on echelon wrench folds (termed  
1073 PSE-1-structures in the description above; see (Cloos, 1928; Riedel, 1929;  
1074 Tchalenko, 1970; Wilcox et al., 1973). *Én echelon folds (corresponding to PSE-1-  
1075 structures) first first* became visible, to be succeeded by and the development of  
1076 Riedel- and P-shears. (R'-shears were subdued as expected for sand-dominated  
1077 sequences (Dooley & Schreurs, 2012). Continued shear followed by collapse and  
1078 interaction between Riedel and P-shears and the subsequent development of Y-  
1079 shears initiated push-up- and flower-structures with N-S-axes (PSE-2), structures  
1080 that were expressed as non-cylindrical (double-plunging) anticlines on the  
1081 surface (e.g. Tchalenko, 1970; Naylor et al., 1986). Structures similar to the PSE-

Formatted: Font: Italic

Formatted: Font: Italic

1082 2-structures that were initiated in the present experiments have previously been  
1083 reported from similar experiments with viscous basal layers covered by sand (e.g.  
1084 Richard et al., 1991; Dauteuil & Mart, 1998), ~~and illustrating the influence of a~~  
1085 ~~mechanical stratified sequence on fold configurations. may have contributed to~~  
1086 ~~the more complex fold systems along the Knølegga Fault Complex.~~

1087  
1088 The Knølegga Fault ~~ZoneComplex~~ occupies a km-wide zone. The master fault  
1089 strand is paralleled by faults with significant normal throws on its hanging wall  
1090 side and ~~these isare~~ considered to be strands belonging to the larger Knølegga  
1091 Fault Complex (EBF; Eastern Boundary Fault; Giannenas, 2018; **Figure 12A**). The  
1092 EBF zone is a top-west normal fault with maximum throw of nearly 2000 m (3000  
1093 meters). It can be followed along its strike for more than 60 km and seems to die  
1094 out by horse-tailing at its tip-points. The vicinity of the master faults of the  
1095 Knølegga Fault Complex locally display isolated elongate positive structures  
1096 constrained by steeply dipping faults. These structures sometimes display  
1097 internal reflection patterns that seem exotic or suspect in comparison to the  
1098 surrounding sequences. Some of these structures resemble positive flower  
1099 structures or push-ups or define narrow anticlines. They are found in both the  
1100 footwall and hanging wall of the border faults and strike parallel to those and the  
1101 axes of these structures parallel the master faults. The traces of such structures  
1102 can be followed over shorter distances than the master faults, and do not occur in  
1103 the central parts of the Vestbakken Volcanic Province. We speculate that these are  
1104 rare fragments of dismembered [PSEEPS-12](#)-type structures.

1105  
1106 Due to the right-stepping geometry during dextral shear in segment 2, the  
1107 southern and northern parts were in the releasing and restraining bend positions,  
1108 respectively (e.g., Christie-Blick & Biddle, 1985). Hence, the southern part of  
1109 segment 2 was subject to oblique extension, subsidence and basin formation when  
1110 the northern part was subject to oblique contraction, shortening and uplift. The  
1111 southern segment expanded to the east and northeast by footwall collapse and  
1112 activation of rotating fault blocks that contributed to a basin floor topography that  
1113 affected the pattern of sediment accumulation (**Figure 9A, B**). The crests of the  
1114 rotating fault blocks are termed PSE-3-structures above, and such eroded fault

1115 block crests are defining the footwalls of major faults in the Vestbakken Volcanic  
1116 Province, providing space for sediment accumulation in the footwalls. The area  
1117 that was affected by the basin formation in the extensional shear duplex stage  
1118 seems to have remained the deepest part of the Vestbakken Volcanic Province,  
1119 whereas the part formed in basin widening by sequential footwall collapse created  
1120 a shallower sub-platform (*sensu* Gabrielsen, 1986) (**Figure 11**). It is expected that  
1121 (regional) basin and (local) fault block subsidence became accelerated during  
1122 phase 2 (extension), and more so in the orthogonal extension experiments  
1123 (BarMar 6) than in the experiments with oblique extension (BarMar 8), but due to  
1124 stabilization of basins by infilling of sand, this was not documented. The widening  
1125 occurred mainly by fault-controlled collapse of the footwalls, and dominantly  
1126 along the master faults that corresponded to the Knølegga Fault ~~Zone~~Complex, but  
1127 also new intra-basinal cross-faults that were initiated in the shear stage (see  
1128 above) became reactivated, contributing to the complexity of the basin  
1129 topography. ~~Referring the reflection seismic data from the Barents Shear Margin,~~  
1130 ~~It is not likely that a stage was reached where all (pull-apart) basin units along~~  
1131 ~~the margin became fully linked, although sedimentary communication along the~~  
1132 ~~margin may have become established is likely.~~

1133  
1134 The contraction (phase 3) clearly reactivated normal faults, probably causing  
1135 focusing of hanging wall strain and folding, rotation of fault blocks and steepening  
1136 of faults. This means that both intra-basinal and marginal faults in the Vestbakken  
1137 Volcanic Province can have suffered late steepening. Contraction expressed as fold  
1138 systems with fold axes paralleling the basin margins development seems to  
1139 correspond very well to the observed structural configuration of the Vestbakken  
1140 Volcanic Province. Here pronounced tectonic inversion is focused along the N-S-  
1141 striking basin margins and along some NE-SW-striking faults in the central parts  
1142 of the basin. Pronounced shortening also occurred inside individual reactivated  
1143 fault blocks either by bulging of the entire sedimentary sequence or as trains of  
1144 folds (**Figure 12**).

1145  
1146 The restraining bend configuration in the northern part of segment 2 was  
1147 characterized by increasing contraction across strike-slip fault strands that

1148 splayed out to the northwest from the central part of segment 2 in an early stage  
1149 of dextral shear. This deformation was terminated by the end of phase 1 by  
1150 stacking of oblique contraction faults (PSE-5 and PSE-64-structures), defining an  
1151 antiformal stack-like structure. This type of deformation falls outside the main  
1152 area, but to the north this type of oblique shortening during the Eocene (phase 1)  
1153 was accommodated by regional-scale strain partitioning (Leever et al., 2011a,b).

1154  
1155 The Vestbakken Volcanic Province is characterized by extensive regional  
1156 shortening. Onset of this event of inversion/contraction is dated to early Miocene  
1157 (Jebsen & Faleide, 1998, Giennenas, 2018) and this deformation included two  
1158 main structural fold styles. The first includes upright to steeply inclined closed to  
1159 open anticlines that are typically present in the hanging wall of master faults.  
1160 These folds typically have wavelengths in the order of 2.5 to 4.5 kilometers, and  
1161 amplitudes of several hundred meters. Most commonly they appear with head-on  
1162 snakehead-structures and are interpreted as buckle folds, albeit a component  
1163 shear may occur in the areas of the most intense deformation, giving a snake-head-  
1164 type geometry. The second style includes gentle to open anticline-syncline pairs  
1165 with upright or steep to inclined axial planes ~~open anticlines-synclines~~ with  
1166 wavelengths in the order of 5 to 7 kilometers and amplitudes of several tens of  
1167 meters to several hundred meters. We associate those with the PSE-4-type  
1168 structures as defined in the BarMar-experiments, ~~These where~~ folds ~~of the former~~  
1169 ~~type~~ are situated in positions ~~where~~ sedimentary sequences have been pushed  
1170 against buttresses provided by master faults along the basin margins, ~~The PSE-6~~  
1171 ~~foldsw~~ ~~whereas the latter type was~~ developed as fold trains in the interior basins,  
1172 where buttressing against larger fault walls was uncommon. Also, this pattern fits  
1173 well with the development and geometry seen in the BarMar-experiments, where  
1174 folding started in the central parts of the closing basins before folding of the  
1175 marginal parts of the basin. In the closing stage the folding and inversion of master  
1176 faults remained focused along the basin margins.

1177  
1178 The experiments clearly demonstrated that contraction by buckle folding was the  
1179 main shortening mechanism of the margin-parallel basin system generated in  
1180 phase 2 (orthogonal or oblique extension) in all segments. In the Vestbakken

1181 Volcanic Province segments of the Knølegga Fault ~~ZoneComplex~~, the EBF and the  
1182 major intra-basinal faults contain clear evidence for tectonic inversion, whereas  
1183 this is less pronounced in others. The hanging wall of the EBF is partly affected by  
1184 fish-hook-type inversion anticlines (Ramsey & Huber, 1987; Griera et al., 2018)  
1185 (**Figure 2D, E**), or isolated hanging wall anticlines or pairs or trains of synclines  
1186 and anticlines (e.g., Roberts, 1989; Coward et al., 1991; Cartwright, 1989; Mitra,  
1187 1993; Uliana et al., 1995; Beauchamp et al. 1996; Gabrielsen et al. 1997; Henk &  
1188 Nemcok 2008), the fold style and associated faults probably being influenced by  
1189 the orientation and steepness of the pre-inversion fault (Williams et al., 1989;  
1190 Cooper et al., 1989; Cooper & Warren, 2010). Some structures of this type can still  
1191 be followed for many kilometers having consistent geometry and attitude. These  
1192 structures have not been much modified by reactivation and are invariably found  
1193 in the proximal parts footwalls of master faults, suggesting that these are  
1194 inversion structures that correlate to PSEEPS-type 5-structures in the  
1195 experiments developed in areas of focused contraction along pre-existing fault  
1196 scarps during OligMiocene inversion.

1197  
1198 Trains of folds with smaller amplitudes and higher frequency are sometimes  
1199 found in fault blocks in the central part of the Vestbakken Volcanic Province  
1200 (**Figure 12F**). Although these structures are not dateable ~~my~~ seismic  
1201 stratigraphical methods (on-lap configurations etc.) we regard these fold strains  
1202 to be correlatable with the tight folds generated in the inversion stage in the  
1203 experiments (PSEEPS-65-structures) and that they are contemporaneous with the  
1204 PSEEPS type\_5-structures.

1205  
1206 Segment 1 in the experiments, ~~that~~which corresponds to the Senja Shear Margin  
1207 segment, displays a structural pattern that is a hybrid between segments 1 and 2.  
1208 It contains incipient structural elements that were developed in full in segments 2  
1209 and 3. segment 2 being dominated by releasing and restraining bend  
1210 configurations and segment 3 dominated by neutral shear. Due to internal  
1211 configurations, the three segments were affected to secondary (oblique) opening  
1212 and contraction in various fashions. Understanding these differences was much  
1213 promoted by the comparison of seismic and model data. ~~is a blend done between~~

1214 ~~configurations done in segments 1 and 2, and the general conclusions drawn~~  
1215 ~~above are valid for this part of the shear margin.~~

1216

## 1217 **Summary and conclusions**

1218

1219 The Barents Shear Margin is a challenging target for structural analysis both  
1220 because it represents a geometrically complex structural system with a multistage  
1221 history, but also because high-quality (3D) ~~seismic~~ reflection ~~seismic~~-data are  
1222 limited and many structures and sedimentary systems generated in the earlier  
1223 tectono-thermal stages have been overprinted and obliterated by younger events.  
1224 This makes analogue experiments very useful in the analysis, since they offer a  
1225 template for what kind of structural elements can be expected. By constraining the  
1226 experimental model according to the outline of the margin geometry and imposing  
1227 a dynamic stress model in harmony according to the state-of-the-art knowledge  
1228 about the regional tectono-sedimentological development, we were able to  
1229 interpret the observations done in ~~seismic~~ reflection ~~seismic~~-data in a new light.

1230

1231 Our observations confirmed that the main segments of the Barents Shear Margin,  
1232 albeit undergoing the same regional stress regime, display contrasting structural  
1233 configurations.

1234

1235 The deformation in segment 2 in the BarMar-experiments, was determined by  
1236 releasing and restraining bends in the southern and northern parts, respectively.  
1237 Thus, the southern part, corresponding to the Vestbakken Volcanic Province, was  
1238 dominated by the development of a regional-scale extensional shear duplex-~~as~~  
1239 ~~defined by Woodcock & Fischer (1983) and Twiss & Moores (2007).~~ By continued  
1240 shear the basin developed into a full-fledged pull-apart basin or rhomb graben  
1241 ~~(Crowell, 1974; Aydin & Nur, 1982)~~ in which rotating fault blocks were trapped.  
1242 The pull-apart-basin became the nucleus for greater basin systems to develop in  
1243 the following phase of extensional ~~and~~ also provid~~ing~~ed the space for folds to  
1244 develop in the contractional phase.

1245

1246 We conclude that fault- and fold systems found in the realm of the Vestbakken  
1247 Volcanic Province are in accordance with a three-stage development that includes  
1248 dextral shear ~~followed by; (oblique)~~ extension and contraction ~~(325/145°)~~ along  
1249 a shear margin with composite geometry.

1250 Folds with NE-SW-trending fold axes ~~that~~ are dominant in wider area of the  
1251 Vestbakken Volcanic Province and are dominated by folds in the hanging walls of  
1252 (older) normal faults, sometimes characterized by narrow, snake-head- or  
1253 harpoon-type structures that are typical for tectonic inversion ~~(Cooper et al.,  
1254 1989; Coward, 1994; Allmendinger, 1998; Yameda & McClay, 2004; Pace &  
1255 Calamitra, 2014)~~ typical of inverted faults.

1256  
1257 Comparing seismic mapping and analogue experiments it is evident that a main  
1258 challenge in analyzing the structural pattern in shear margins of complex  
1259 geometry and multiple reactivation is the low potential for preservation of  
1260 structures that were generated in the earliest stages of the development.

1261

#### 1262 **Author contribution**

1263 R.H. Gabrielsen: Contributions to outline, design and performance of experiments.

1264 First writing and revisions of manuscript. First drafts of figures.

1265 P.A. Giennenas: Seismic interpretation in the Vestbakken Volcanic Province.

1266 Identification and description of fold families.

1267 ~~Suggestion:~~

1268 D. Sokoutis: Main responsibility for set-up, performance and handling of  
1269 experiments. Revisions of manuscript.

1270 E. Willigshofer: Performance and handling of experiments. Revisions of  
1271 manuscript. Design and revisions of figure material.

1272 Md. Hassaan: Background seismic interpretation. Discussions and revisions of  
1273 manuscript. Design and revisions of figure material.

1274 J.I. Faleide: Regional interpretations and design of experiments. Participation in  
1275 performance and interpretations of experiments. Revisions of manuscript, design  
1276 and revisions of figure material.

1277

1278

Formatted: Not Superscript/ Subscript

1279

1280 **Acknowledgements**

1281 The work was supported by ARCEX (Research Centre for Arctic Petroleum  
1282 Exploration), which was funded by the Research Council of Norway (grant number  
1283 228107) together with 10 academic and six industry (Equinor, Vår Energi, Aker  
1284 BP, Lundin Energy Norway, OMV and Wintershall Dea) partners. Muhammad  
1285 Hassaan was funded by the Suprabasins project (Research Council of Norway  
1286 grant no. 295208). We thank to Schlumberger for providing us with academic  
1287 licenses for Petrel software to do seismic interpretation. Two anonymous  
1288 reviewers and the editors of this special volume provided comments, suggestions  
1289 and advice that enhanced the clarity and scientific quality of the paper.

1290

1291 **FIGURES**

1292

1293 **Figure 1:** **A)** The Barents Sea provides is separated from the Norwegian-  
1294 Greenland Sea by the ~~d~~De Geer ~~Zone-transfer margin linking the North Atlantic to~~  
1295 ~~the Arctic Eurasia Basin~~. Red box shows the present study area. **B)** Structural map  
1296 Barents Sea shear margin. Note segmentation of the continent-ocean transition.  
1297 Abbreviations (from north to south): ~~WSFTB = West Spitsbergen Fold-and-Thrust~~  
1298 ~~Belt~~, ~~HFZ = Hornsund Fault ZoneComplex Zone~~, ~~KFZG = Knølegga Fault~~  
1299 ~~ZoneComplex~~, ~~VVP = Vestbakken Volcanic Province~~, ~~SB = Sørvestsnaget Basin~~, ~~VH~~  
1300 ~~= Veslemøy High~~, ~~SR = Senja Ridge~~, ~~SSMFZ = Senja Shear Margin Zone~~, ~~SR = Senja~~  
1301 ~~Ridge~~, ~~SB = Sørvestsnaget Basin~~, ~~VVP = Vestbakken Volcanic Province~~. Blue lines  
1302 indicate position of seismic profiles in Figure 2 and red line in Figure 1B-X-X' shows  
1303 the western limitation border of the thinned crust (see also Figure 3). Chron  
1304 numbers are indicated on oceanic crust area.

1305

1306 **Figure 2:** Seismic examples from various segments of the Barents Sea shear  
1307 margin, Vestbakken Volcanic Province. **A)** Gentle, partly collapsed NE-SW-striking  
1308 anticline/dome of fold family 1 (Giannenas 2018) of uncertain origin in the  
1309 eastern terrace domain of the southern Vestbakken Volcanic Province. The origin  
1310 of this structure is obscure, but one can speculate that some of the open syncline-  
1311 anticline pairs originated as PSE-1-structures. This may be a remnant, rotated  
1312 PSE-1 structure (see text for explanation). **B,C)** Flower (PSE-2)-structure in area  
1313 dominated by neutral shear. **C)** Section through push-up (PSE-4-structure)  
1314 associated with restraining bend. **D-E)** Assymetrical folds (fold family 2;  
1315 Giannenas 2019) situated along the eastern margin of the Vestbakken Volcanic  
1316 Province. These may representing primary SPSE-545-structures. These  
1317 structures are focused in the hangingwalls along the escarpments margins of  
1318 master fault blocks, representing or reactivated SPE-2 structures. **DF)** Trains of  
1319 symmetrical folds with upright fold axes (corresponding to PSE-56-structures  
1320 family) are preserved inside larger fault blocks. See Table 1 and text for  
1321 explanation of the SPSE-structures. **E)** Section through push up associated with  
1322 restraining bend (PSE-4-structure). **F)** Flower (PSE-2)-structure in aera  
1323 dominated by neutral shear.

1324

1325

1326 **Figure 3:** **A)** Schematic set-up of BarMar3-experiment as seen in map view. **B)**  
1327 Section through same experiment before deformation, indicating stratification  
1328 and thickness relations. **C)** Standard positions and orientation for sections cut in  
1329 all experiments in the BarMar-series. Yellow numbers are section numbers. Black  
1330 numbers indicate angle between the margins of the experiment (relative to N-S)  
1331 for each profile. **D)** Outline of silicone putty layer as applied in all experiments.  
1332 Inset shows original structural map of the Barents Margin used to define the width  
1333 of the thinned crust (same as Fig. 1B). Red line (X-X') indicates the western limit  
1334 of the thinned zone.

1335

1336 **Figure 4:** Position of segments and major structural elements as referred to in the  
1337 text and subsequent figures (see particularly Figures 5 and 6). This example is  
1338 taken from the reference experiment BarMar6. All experiments BarMar6-9  
1339 followed the same pattern, and the same nomenclature was used in the

Formatted: Font color: Text 1

Formatted: Font color: Text 1

Formatted: Font color: Auto

Formatted: Font: Bold, Font color: Text 1

Formatted: Font color: Text 1

Formatted: Font: Bold

Formatted: Font: Bold

Formatted: Font: Bold

1340 description of [all experiments and provides the template for the definition of](#)  
1341 [structural elements in Figure 7, these experiments.](#)

1342

1343 **Figure 5:** Sequential development of experiment BarMar6 by 0.5, 2.4, 3.5, 4.0 and  
1344 5.0 cm of dextral shear (Steps A-E), orthogonal extension (steps F-H) and oblique  
1345 contraction (steps I-J). The master fault strands are numbered in **Figure 4**, and  
1346 the sequential development for each structural family is shown in **Figure 7**.

1347

1348 **Figure 6:** Sequential development of experiment BarMar8 by ~~1.0, 2.4, 3.5, 4.0~~  
1349 and 5.0 cm of dextral shear (Steps A-~~E~~C), oblique extension (steps ~~F~~D-~~H~~F) and  
1350 oblique contraction (steps ~~G~~-I-J). ~~Step J represents the final model after end of~~  
1351 ~~contraction.~~ The master fault strands are numbered in **Figure 3**, and the  
1352 sequential development for each structural family is shown in **Figure 7**. Phases 2  
1353 and 3 involved oblique (325°) extension and contraction in this experiment.

1354

1355 **Figure 7:** Summary of sequential activity in each master structural element  
1356 (**Figure 4**) in Experiment BarMar6 (**Figure 5**). Type and amount of displacement  
1357 is shown in two upper horizontal rows. The vertical blue bar indicates the stage at  
1358 which full along-strike communication became established between marginal  
1359 basins. [Color code \(see in-set\) indicates type of displacement at any stage.](#)

1360

1361 **Figure 8:** PSE-1 anticline-syncline pairs in segment 1 experiment BarMar6 in an  
1362 oblique view. PSE-1 folds were constrained to the very fault zone and the fold axes  
1363 (blue lines) and extended only 3-4 cm beyond the fault zone. PSE-2 structures  
1364 (incipient ~~shear-duplex~~push-ups and positive flower structures; yellow lines)  
1365 were delineated by shear faults and completely cannibalized PSE-1 structures by  
1366 continued shear. Yellow and blue lines show the rotation of the fold axial trace  
1367 caused by dextral shearing of c. 1.5 cm. 25mm of dextral shear. By a displacement  
1368 of 35mm the remains of the PSE-1 structure was completely obliterated. The  
1369 distance between the markers (dark lines) is 5cm. Yellow arrow marks north-  
1370 direction.

1371 White arrows indicate shear direction.

1372

1373

1374 **Figure 9:** Cross-sections through PSE-2-related structures. **A)** Folded core of  
1375 incipient push-up/positive flower structure in segment 1, experiment BarMar6.  
1376 The fold structure is completely enveloped of shear faults that have a twisted  
1377 along-strike geometry. Note that the eastern margin of the structure developed  
1378 into a negative structure at a late stage in the development (filled by black-pink  
1379 sand sequence) and that the silicone putty sequence (basal pink sequence) was  
1380 entirely isolated in the footwall. **B)** Similar structure in experiment BarMar8. The  
1381 weak silicone putty layer here bridged the high-strain zone and focused folding  
1382 that propagated into the sand layers (blue). The folds in upper (pink layers) were  
1383 associated with the contractional stage, because they contributed to a surface  
1384 relief filled in by red-black-sand sequence that was sieved into the margin during  
1385 the contractional stage. **C)** Contraction associated with "crocodile structure" in the  
1386 footwall of the main fault in segment 1, experiment BarMar8. Note disharmonic  
1387 folding with contrasting fold geometries in hanging wall and footwall and at  
1388 different stratigraphic levels in the footwall, indicating shifting stress situation in

1389 time and space in the experiment. **D)** Transitional fault strand between to more  
1390 strongly sheared fault segments (experiment BarMar9).

1391  
1392  
1393 **Figure 10: A)** contrasting structural styles along the master fault system in  
1394 segment 2 in map view and **(B)** cross sections of experiment BarMar9. SL denotes  
1395 silicone layer, the stippled line the boundary between pre-and syn-deformation  
1396 layers and the white dashed line the boundary with the post-deformation layers.

1397  
1398  
1399 **Figure 11:** Nine stages in the development of the extensional shear duplex system  
1400 above the releasing bend in experiment BarMar9. The master faults that  
1401 developed at an incipient stage (e.g. Fault 3 that constrained the eastern margin  
1402 of the extensional shear duplex) remained stable and continued to be active  
1403 throughout the experiment (Figure 7), but became overstepped by faults in its  
1404 footwall that became the basin contraction faults at the later stages H and I. Note  
1405 that the developing basement was stabilized by infilling of gray sand during this  
1406 part of the experiment. Note that Fault 3 remained active and broke through the  
1407 basin infill also after the basin infill overstepped the original basin margin. The  
1408 distance between the markers (dark lines) is 5cm. -Yellow arrow marks north-  
1409 direction. Note that figure I has a different orientation.

1410  
1411 **Figure 12:** PSE-5- and PSE-6 folds generated during phase 3-inversion,  
1412 experiment BarMar8. Note that fold axes mainly parallel the basin rims, but that  
1413 they deviate from that in the central parts of the basins in some cases. Note that  
1414 the folds are best developed in segment 2, which accumulated extension in the  
1415 combined shear and extension stages.

1416  
1417  
1418 **Figure 13;** Main stages in opening of the North Atlantic. A) Present day. B) chron  
1419 5 (10 Ma in the late Miocene). C) chron 13 (33 Ma in the earliest Oligocene). D)  
1420 chron 24 (53 Ma in the early Eocene).

1421  
1422

1423  
1424  
1425  
1426  
1427  
1428  
1429  
1430  
1431  
1432  
1433  
1434  
1435  
1436  
1437  
1438  
1439  
1440  
1441  
1442  
1443  
1444  
1445  
1446  
1447  
1448  
1449  
1450  
1451  
1452  
1453  
1454  
1455  
1456  
1457  
1458  
1459  
1460  
1461  
1462  
1463  
1464  
1465  
1466  
1467  
1468  
1469  
1470

## References

- Allemand, P. & Brun, J. P., 1991: Width of continental rifts and rheological layering of the lithosphere. *Tectonophysics*, 188, 63-69, 1991.
- Allmendinger, R. W., 1998: Inverse and forward numerical modeling of threeshear fault-propagation folds, *Tectonics*, 17(4), 640-656, 1998.
- Auzemery, A., ~~E.~~ Willingshofer, ~~E.~~ D., Sokoutis, ~~D.~~ J.P., Brun, ~~J. P.~~, and ~~S.A.P.L.~~ Cloetingh, ~~S. A. P. L.~~, 2021: Passive margin inversion controlled by stability of the mantle lithosphere, *Tectonophysics*, 817, 229042, 1-17, <https://doi.org/10.1016/j.tecto.2021.229042>, 2021.
- Aydin, A. & Nur, A., 1982: Evolution of pull-apart basins and their scale independence. *Tectonics*, 1, 91-105, 1982.
- Ballard, J.-F., Brun, J.-P., & Van Ven Driessche, J., 1987: Propagation des chevauchements au-dessus des zones de décollement: modèles expérimentaux. *Comptes Rendus de l'Académie des Sciences, Paris*, 11, 305, 1249-1253, 1987.
- Basile, C., 2015: Transform continental margins – Part 1: Concepts and models. *Tectonophysics*, 661, pp.1-10. doi: 10.1016/j.tecto.2015.08.034, 2015.
- Basile, C. & Brun, J.-P., 1997: Transtensional faulting patterns ranging from pull-apart basins to transform continental margins: an experimental investigation, *Journal of Structural Geology*, 21, 23-37, 1997.
- Beauchamp, W., Barazangi, M., Demnati, A., & El Alji, M., 1996: Intracontinental rifting and inversion: Missouri Basin and Atlas Mountains, Morocco. *American Association of Petroleum Geologists Bulletin*, 80(9), 1455-1482, 1996.
- Bergh, S. G., Braathen, A., & Andresen, A., 1997: Interaction of basement-involved and thin-skinned tectonism in the Tertiary fold-and-thrust belt of Central Spitsbergen, Svalbard. *American Association of Petroleum Geologists Bulletin*, 81(4), 637-661, 1997.
- Bergh, S. G. & Grogan, P., 2003: Tertiary structure of the Sørkapp-Hornsund Region, South Spitsbergen, and implications for the offshore southern extension of the fold-thrust-belt. *Norwegian Journal of Geology*, 83, 43-60, 2003.
- Biddle, K. T. & Christie-Blick, N., (eds.), 1985a: Strike-Slip Deformation, Basin Formation, and Sedimentation: Society of Economic Paleontologists and Mineralogists Special Publication, 37, 386 pp, 1985a.
- Biddle, K. T. & Christie-Blick, N., 1985b: Glossary — Strike-slip deformation, basin formation, and sedimentation, in: Biddle, K. T., and Christie-Blick, N. (eds.): *Strike-Slip Deformation, Basin Formation, and Sedimentation: Society of Economic Paleontologists and Mineralogists Special Publication*, 37, 375-386, 1985b.
- Blaich, O. A., Tsikalas, F., & Faleide, J. I., 2017: New insights into the tectono-

1471 stratigraphic evolution of the southern Stappen High and the transition to Bjørnøya  
1472 Basin, SW Barents Sea, Marine and Petroleum Geology, 85, 89-105, doi:  
1473 10.1016/j.marpetgeo.2017.04.015, [2017](#).  
1474  
1475 Breivik, A. J., Faleide, J. I., [and](#) Gudlaugsson, S. T., [1998](#): Southwestern Barents Sea  
1476 margin: late Mesozoic sedimentary basins and crustal extension, Tectonophysics, 293,  
1477 21-44, [1998](#).  
1478  
1479 Breivik, A. J., Mjelde, R., Grogan, P., Shinamura, H., Murai, Y., [and](#) Nishimura, Y.,  
1480 [2003](#): Crustal structure and transform margin development south of Svalbard based on  
1481 ocean bottom seismometer data. Tectonophysics, 369, 37-70, [2003](#).  
1482  
1483 Brekke, H., [2000](#): The tectonic evolution of the Norwegian Sea continen- tal margin  
1484 with emphasis on the Vøring and Møre basins: Geological Society, London, Special  
1485 Publication, 136, 327–378, [2000](#).  
1486  
1487 Brekke, H. [and](#) Riis, F., [1987](#): Mesozoic tectonics and basin evolution of the  
1488 Norwegian Shelf between 60°N and 72°N. Norsk Geologisk Tidsskrift, 67, 295-322,  
1489 [1987](#).  
1490  
1491 Burchfiel, B. C. [and](#) Stewart, J. H., [1966](#): "Pull-apart" origin of the central segment of  
1492 Death Valley, California. Geological Society of America Bulletin., 77, 439-442, [1966](#).  
1493  
1494 Campbell, J. D., [1958](#): *En échelon* folding, *Economical Geology*, 53(4), 448-472, [1958](#).  
1495  
1496 Cartwright, J. A., [1989](#): The kinematics of inversion in the Danish Central Graben. in:  
1497 M.A.Cooper & G.D.Williams (eds.): *Inversion Tectonics*. Geological Society of  
1498 London Special Publication, 44, 153-175, [1989](#).  
1499  
1500 Casas, A. M., Gapals, D., Nalpas, T., Besnard, K., [and](#) Román-Berdiel, T., [2001](#):  
1501 Analogue models of transpressive systems, *Jornal of Structural Geology*, 23,733-743,  
1502 [2001](#).  
1503  
1504 Christie-Blick, N. [and](#) Biddle, K. T., [1985](#): Deformation and basin formation along  
1505 strike-slip faults. in: Biddle, K.T. & Christie-Blick, N. (eds.): *Strike-slip deformation,*  
1506 *basin formation and sedimentation*. Society of Economic Mineralogists and  
1507 Palaeontologists (Tulsa Oklahoma), Special Publication, 37, 1-34, [1985](#).  
1508  
1509 Cloos, H., [1928](#): Experimenten zur inneren Tectonick, *Zentralblatt für Mineralogie,*  
1510 *Geologie und Palaentologie*, 1928B, 609-621, [1928](#).  
1511  
1512 Cloos, H., [1955](#): Experimental analysis of fracture patterns, *Geological Society of*  
1513 *America Bulletin*, 66(3), 241-256, [1955](#).  
1514  
1515 Cooper, M. [and](#) Warren, M. J., [2010](#): The geometric characteristics, genesis and  
1516 petroleum significance of inversion structures, in Law, R.D., Butler, R.W.H.,  
1517 Holdsworth, R.E., Krabbendam, M. & Strachan, R.A. (eds.): *Continental Tectonics and*  
1518 *Mountain Building: The Lagacy of Peache and Horne*, Geological Society of London,  
Special Publication, 335, 827-846, [2010](#).

1519 Cooper, M. A., Williams, G. D., de Graciansky, P. C., Murphy, R. W., Needham, T.,  
1520 de Paor, D., Stoneley, R., Todd, S. P., Turner, J. P. & Ziegler, P. A., 1989: Inversion  
1521 tectonics – a discussion. Geological Society, London, Special Publications, 44, 335-  
1522 347, 1989.

1523

1524 Coward, M., 1994: Inversion tectonics, in: Hancock, P.L. (ed.): Continental  
1525 Deformation, Pergamon Press, 289-304, 1994.

1526

1527 Coward, M. P., Gillcrist, R. & Trudgill, B., 1991: Extensional structures and their  
1528 tectonic inversion in the Western Alps, in: A.M.Roberts, G.Yielding & B.Freeman  
1529 (eds.): The Geometry of Normal Faults. Geological Society of London Special  
1530 Publication, 56, 93-112, 1991.

1531

1532 Crowell, J., 1962: Displacement along the San Andreas Fault, California, Geological  
1533 Society of America Special Papers, 71, 59pp, 1962.

1534

1535 Crowell, J. C., 1974a: Origin of late Cenozoic basins in southern California. in R.H.Dorr  
1536 & R.H.Shaver (eds.): Modern and ancient geosynclinal sedimentation. SEPM Special  
1537 Publication, 19, 292-303, 1974a.

1538

1539 Crowell, J. C., 1974b: Implications of crustal stretching and shortening of coastal  
1540 Ventura Basin, in: Howell, D.G. (ed.): Aspects of the geological history of the  
1541 California continental Borderland, American Association of Petroleum Geologists,  
1542 Pacific Section, Publication 24, 365-382, 1974b.

1543

1544 Cunningham, W. D. & Mann, P. (eds.), 2007a: Tectonics of Strike-Slip Restraining  
1545 and Releasing Bends, Geological Society London Special Publication, 290, 482pp.  
1546

1547 Cunningham, W. D. & Mann, P., 2007b: Tectonics of Strike-Slip Restraining and  
1548 Releasing Bends, in: Cunningham, W.D. & Mann, P. (eds.), 2007: Tectonics of Strike-  
1549 Slip Restraining and Releasing Bends, Geological Society London Special Publication,  
1550 290, 1-12, 2007b.

1551

1552 Dauteuil, O. & Mart, Y., 1998: Analogue modeling of faulting pattern, ductile  
1553 deformation, and vertical motion in strike-slip fault zones, Tectonics, 17(2), 303-310,  
1554 1998.

1555

1556 Del Ventisette, C., Montanari, D., Sani, F., Bonini, M., and Corti, G., 2007: Reply to  
1557 comment by J. Wickham on ‘‘Basin inversion and fault reactivation in laboratory  
1558 experiments’’. Journal of Structural Geology 29, 1417–1418, 2007.

1559

1560 Dooley, T. & McClay, K., 1997: Analog modeling of pull-apart basins, American  
1561 Association of Petroleum Geologists Bulletin, 81(11), 1804-1826, 1997.

1562

1563 Dooley, T. P. & Schreurs, G., 2012: Analogue modelling of intraplate strike-slip  
1564 tectonics: A review and new experimental results, Tectonophysics, 574-575, 1-71,  
1565 2012.

1566

1567 Doré, A.G. & Lundin, E.R., 1996: Cenozoic compressional structures on the NE  
1568 Atlantic margin: nature, origin and potential significance for hydrocarbon exploration.  
1569 *Petroleum Geosciences*, 2, 299-311, 1996.

1570  
1571 Doré, A.G., Lundin, E.R., Gibbons, A., Sømme, T.O. & Tørudbakken, B.O.,  
1572 2016: Transform margins of the Arctic: a synthesis and re-evaluation *in*: Nemcok, M.,  
1573 Rybár, S., Sinha, S.T., Hermeston, S.A. & Ledvényiová, L. (eds.): *Transform Margins:*  
1574 *Development, Control and Petroleum Systems*, Geological Society London, Special  
1575 Publication, 431, 63-94, 2016.

1576  
1577 Doré, A.G., Lundin, E.R., Jensen, L.N., Birkeland, Ø., Eliassen, P.E. & Fichler,  
1578 C., 1999: Principal tectonic events in the evolution of the northwest European Atlantic  
1579 margin. In: A.J.Fleet & S.A.R.Boldy (eds.): *Petroleum Geology of Northwest Europe:*  
1580 *Proceedings of the Fifth Conference* (Geological Society of London), 41-61, 1999.

1581  
1582 Eidvin, T., Goll, R.M., Grogan, P., Smelror, M. & Ulleberg, K., 1998: The  
1583 Pleistocene to Middle Eocene stratigraphy and geological evolution of the western  
1584 Barents Sea continental margin at well site 731675-1 (Bjørnøya West area). *Norsk*  
1585 *Geologisk Tidsskrift*, 78, 99-123, 1998.

1586  
1587 Eidvin, T., Jansen, E. & Riis, F., 1993: Chronology of Tertiary fan deposits off the  
1588 western Barents Sea: Implications for the uplift and erosion history of the Barents Shelf.  
1589 *Marine Geology*, 112, 109-131, 1993.

1590  
1591 Eldholm, O., Faleide, J.I. & Myhre, A.M., 1987: Continent-ocean transition at the  
1592 western Barents Sea/Svalbard continental margin. *Geology*, 15, 1118-1122.

1593  
1594 Eldholm, O., Thiede, J., and Taylor, E., 1989: Evolution of the Vøring volcanic  
1595 margin, *in*: Eldholm, O., Thiede, J., and Taylor, E., (eds.): *Proceedings of the Ocean*  
1596 *Drilling Program, Scientific Results*, 104: College Station (Ocean Drilling Program),  
1597 TX, 1033-1065, 1989.

1598  
1599 Eldholm, O., Tsikalas, F. & Faleide, J.I., 2002: Continental margin off Norway  
1600 62-75°N: Paleogene tectono-magmatic segmentation and sedimentation. *Geological*  
1601 *Society of London Special Publication*, 197, 39-68, 2002.

1602  
1603 Emmons, R.C., 1969: Strike-slip rupture patterns in sand models, *Tectonophysics*, 7,  
1604 71-87, 1969.

1605  
1606 Faugère, E., Brun, J.-P. & Van Den Driessche, J., 1986: Bassins asymétriques en  
1607 extension pure et en détachements: Modèles expérimentaux, *Bulletin Centre Recherche*  
1608 *Exploration et Production Elf Aquitaine*, 10(2), 13-21, 1986.

1609  
1610 Faleide, J.I., Bjørlykke, K. & Gabrielsen, R.H., 2015: Geology of the Norwegian  
1611 Shelf. *in*: Bjørlykke, K.: *Petroleum Geoscience: From Sedimentary Environments to*  
1612 *Rock Physics 2<sup>nd</sup> Edition*, Springer-Verlag, Berlin Heidelberg, Chapter 25, 603 -637,  
1613 2015.

1614  
1615 Faleide, J.I., Myhre, A.M. & Eldholm, O., 1988: Early Tertiary volcanism at the  
1616 western Barents Sea margin. *in*: A.C.Morton & L.M.Parsons (eds.): *Early Tertiary*

1617 volcanism and the opening of the NE Atlantic. Geological Society of London Special  
1618 Publication, 39, 135-146, [1988](#).

1619

1620 Faleide, J. I., Tsikalas, F., Breivik, A. J., Mjelde, R., Ritzmann, O., Engen, Ø., Wilson,  
1621 J., [and](#) Eldholm, O., [2008](#): Structure and evolution of the continental margin off  
1622 Norway and the Barents Sea. *Episodes*, 31(1), 82-91, [2008](#).

1623

1624 Faleide, J. I., Vågnes, E., [and](#) Gudlaugsson, S. T., [1993](#): Late Mesozoic - Cenozoic  
1625 evolution of the south-western Barents Sea in a regional rift-shear tectonic setting.  
1626 *Marine and Petroleum Geology*, 10, 186-214, [1993](#).

1627

1628 Fichler, C. [and](#) Pastore, Z., [2022](#): Petrology and crystalline crust in the southwestern  
1629 Barents Sea inferred from geophysical data. *Norwegian Journal of Geology*, 102, 41pp,  
1630 <https://dx.doi.org/10.17850/njg102-2-2>, [2022](#).

1631

1632 Freund, R., [1971](#): The Hope Fault, a strike-slip fault in New Zealand, New Zealand  
1633 Geological Survey Bulletin, 86, 1-49, [1971](#).

1634

1635 Gabrielsen, R. H., [1986](#): Structural elements in graben systems and their influence on  
1636 hydrocarbon trap types. in: A.M. Spencer (ed.): *Habitat of Hydrocarbons on the*  
1637 *Norwegian Continental Shelf*. Norw. Petrol. Soc. (Graham & Trotman), 55 – 60, [1986](#).

1638

1639 Gabrielsen, R. H., Færseth, R. B., Jensen, L. N., Kalheim, J. E., [and](#) Riis, F., [1990](#):  
1640 Structural elements of the Norwegian Continental Shelf. Part I: The Barents Sea  
1641 Region. *Norwegian Petroleum Directorate, Bulletin*, 6, 33pp, [1990](#).

1642

1643 Gabrielsen, R. H., Grunnaleite, I., [and](#) Rasmussen, E., [1997](#): Cretaceous and Tertiary  
1644 inversion in the Bjørnøyrenna Fault Complex, south-western Barents Sea. *Marine and*  
1645 *Petroleum Geology*, 14, 165-178, [1997](#).

1646

1647 Gac, S., Klitzke, P., Minakov, A., ~~lexander~~, Faleide, J. I., [and](#) Scheck-Wenderoth, M.,  
1648 [2016](#): Lithospheric strength and elastic thickness of the Barents Sea and Kara Sea  
1649 region, *Tectonophysics*, 691, 120-132, doi: 10.106/j.tecto.2016.04.028, [2016](#).

1650

1651 Gaina, C., Gernigon, L., [and](#) Ball, P., [2009](#): Palaeocene – Recent plate boundaries  
1652 in the NE Atlantic and the formation of the Jan Mayen microcontinent. *Journal of the*  
1653 *Geological Society, London*, 166(4), 601-616, [2009](#).

1654

1655 Ganerød, M., Smethurst, M. A., Torsvik, T. H., Prestvik, T., Rouse, S., McKenna, C.,  
1656 van Hinsbergen, D. J. J., [and](#) Hendriks, W. W. H., [2010](#): The North Atlantic Igneous  
1657 Province reconstructed and its relation to the Plume Generation Zone: the Antrim Lava  
1658 Group revisited. *Geophysical Journal International*, 182, 183-202, doi: 10.1111/j.1365-  
246X.2010.04620.x, [2010](#).

1659

1660 Giennenas, P. A., [2018](#): The Structural Development of the Vestbakken Volcanic  
1661 Province, Western Barents Sea. Relation between Faults and Folds, Unpubl. Master  
1662 thesis, University of Oslo [2018](#), 89 pp, [2018](#).

1663

1664 Graymer, R. W., Langenheim, V. E., Simpson, R. W., Jachens, R. C., [and](#) Ponce, D.  
A., [2007](#): Relative simple through-going fault planes at large-earthquake depth may be

1665 concealed by surface complexity of strike-slip faults, *in*: Cunningham, W.D. & Mann, P.  
 1666 (eds.): *Tectonics of Strike-Slip Restraining and Releasing Bends*, Geological Society  
 1667 London Special Publication, 290, 189-201, [2007](#).  
 1668  
 1669 Griera, A., Gomez-Rivas, E., & Llorens, M.-G., [2018](#): The influence of layer-  
 1670 interface geometry of single-layer folding. *Geological Society of London Special*  
 1671 *Publication* 487, SP487:4, [2018](#).  
 1672  
 1673 Grogan, P., Østvedt-Ghazi, A.-M., Larssen, G. B., Fotland, B., Nyberg, K., Dahlgren,  
 1674 S., & Eidvin, T., [1999](#): Structural elements and petroleum geology of the Norwegian  
 1675 sector of the northern Barents sea. *in*: Fleet, A.J. & Boldry, S.A.R. (eds.): *Petroleum*  
 1676 *Geology of Northwest Europe: Proceedings of the 5th Conference*, Geological Society  
 1677 of London, 247-259, [1999](#).  
 1678  
 1679 Groshong, R. H., [1989](#): Half-graben structures: balanced models of extensional  
 1680 fault bend folds, *Geological Society of America Bulletin*, 101, 96-195, [1989](#).  
 1681  
 1682 Gudlaugsson, S. T., & Faleide, J. I., [1994](#): The continental margin between  
 1683 Spitsbergen & Bjørnøya, in: O.Eiken (ed.): *Seismic Atlas of Western Svalbard*, Norsk  
 1684 Polarinstitutt Meddelelser, 130, 11-13, [1994](#).  
 1685  
 1686 Gudlaugsson, S. T., Faleide, J. I., Johansen, S. E., & Breivik, A. J., [1998](#): Late  
 1687 Palaeozoic structural development of the south-western Barents Sea. *Marine and*  
 1688 *Petroleum Geology*, 15, 73-102, [1998](#).  
 1689  
 1690 Hamblin, W. K., [1965](#): Origin of "reverse drag" on the down-thrown side of normal  
 1691 faults, *Geological Society of America Bulletin*, 76, 1145-1164, [1965](#).  
 1692  
 1693 Hanisch, J., [1984](#): The Cretaceous opening of the Northeast Atlantic. *Tectonophysics*,  
 1694 101, 1-23, [1984](#).  
 1695  
 1696 Harding, T. P., [1974](#): Petroleum traps associated with wrench faults. *American*  
 1697 *Association of Petroleum Geologists Bulletin*, 58, 1290-1304, [1974](#).  
 1698  
 1699 Harding, T. P. & Lowell, J. D., [1979](#): Structural styles, their plate tectonic habitats,  
 1700 and hydrocarbon traps in petroleum provinces, *American Association of Petroleum*  
 1701 *Geologists Bulletin*, 63, 1016-1058, [1979](#).  
 1702  
 1703 Harland, W. B., [1965](#): The tectonic evolution of the Arctic-North Atlantic Region, in:  
 1704 Taylor, J.H., Ruttan, M.G., Hales, A.L., Shackleton, R.M., Nairn, A.E. & Harland, W.B.,  
 1705 Discussion, A Symposium on Continental Drift, *Philosophical Transactions of the*  
 1706 *Royal Society of London*, Series A, 258, 1088, 59-75, [1965](#).  
 1707  
 1708 Harland, W. B., [1969](#): Contributions of Spitsbergen to understanding of tectonic  
 1709 evolution of North Atlantic Region, *American Association of Petroleum Geologists*,  
 1710 *Memoir* 12, 817-851, [1969](#).  
 1711  
 1712 Harland, W. B., [1971](#): Tectonic transpression in Caledonian Spitsbergen, *Geological*  
 1713 *Magazine*, 108, 27-42, [1971](#).  
 1714

1715 Henk, A. & Nemcok, M., 2008: Stress and fracture prediction in inverted half-  
1716 graben structures. *Journal of Structural Geology*, 30(1), 81-97, [2008](#).

1717 Horni, J. Á., Hopper, J. R., Blischke, A., Geisler, W. H., Stewart, M., Mcdermott, K.,  
1718 Judge, M., Erlendsson, Ö. & Ártíng, U. E., 2017: Regional Distribution of  
1719 Volcanism within the North Atlantic Igneous Province. *The NE Atlantic Region: A*  
1720 *Reappraisal of Crustal Structure, Tectonostratigraphy and Magmatic Evolution*.  
1721 Geological Society, London, Special Publications, 447, 105-125,  
1722 <https://doi.org/10.1144/SP447.18>, [2017](#).

1723 Horsfield, W. T., 1977: An experimental approach to basement-controlled faulting.  
1724 *Geologie en Mijbouw*, 56(4), 3634-370, [1977](#).

1725  
1726 Hubbert, M. K., 1937: Theory of scale models as applied to the study of geologic  
1727 structures, *Bulletin Geological Society of America*, 48, 1459-1520, [1937](#).

1728 Jebsen, C. & Faleide, J. I., 1998: Tertiary rifting and magmatism at the western  
1729 Barents Sea margin (Vestbakken volcanic province). III international conference on  
1730 Arctic margins, ICAM III; abstracts; plenary lectures, talks and posters, 92, [1998](#).

1731 Khalil, S. M. & McClay, K. R., 2016: 3D geometry and kinematic evolution of  
1732 extensional fault-related folds, NW Red Sea, Egypt. in: Childs, C., Holdsworth, R. E.,  
1733 Jackson, C. A. L., Manzocchi, T., Walsh, J. J. & Yielding, G. (eds.): *The Geometry and*  
1734 *Growth of Normal Faults*, Geological Society, London, Special Publication 439,  
1735 [doi.org/10.1144/SP439.11](https://doi.org/10.1144/SP439.11), [2016](#).

1736  
1737 Klinkmüller, M., Schreurs, G., Rosenau, M., and Kemnitz, H., 2016: Properties of  
1738 granular analogue model materials: a community wide survey. *Tectonophysics*  
1739 684, 23-38. <http://dx.doi.org/10.1016/j.tecto.2016.01.017>.feb., [2016](#).

1740  
1741 Knutsen, S.-M. & Larsen, K. I., 1997: The late Mesozoic and Cenozoic evolution  
1742 of the Sørvestsnaget Basin: A tectonostratigraphic mirror for regional events  
1743 along the Southwestern Barents Sea Margin? *Marine and Petroleum Geology*,  
1744 14(1), 27-54, [1997](#).

1745  
1746 Kristensen, T. B., Rotevatn, A., Marvik, M., Henstra, G. A., Gawthorpe, R. L. &  
1747 Ravnås, R., 2017: Structural evolution of sheared basin margins: the role of strain  
1748 partitioning. *Sørvestsnaget Basin, Norwegian Barents Sea, Basin Research*, 2017),  
1749 1-23, [doi:10.1111/bre.12235](https://doi.org/10.1111/bre.12235), [2017](#).

1750  
1751 Le Calvez, J.-H. & Vendeville, B. C., 2002: Experimental designs to mode along  
1752 strike-slip fault interaction. *in*: Scellart, W. P. & Passcheir, C. (eds.). *Analogue*  
1753 *Modeling of large-scale Tectonic Processes*, *Journal of Virtual Explorer*, 7, 7-23,  
1754 [2002](#).

1755  
1756 Leever, K. A., Gabrielsen, R. H., Sokoutis, D. & Willingshofer, E., 2011a: The  
1757 effect of convergence angle on the kinematic evolution of strain partitioning in  
1758 transpressional brittle wedges: insight from analog modeling and high resolution

Formatted: Font: 12 pt

Formatted: Font: 12 pt

Formatted: Font: 12 pt

Formatted: Font: +Body (Cambria)

1759 digital image analysis. *Tectonics*, 30, TC2013, 1-25, doi: 10.1029/2009TC002649.  
1760 [2011a](#).

1761

1762 Leevers, K. A., Gabrielsen, R. H., Faleide, J. I. & Braathen, A., ~~2011b~~: A  
1763 transpressional origin for the West Spitsbergen Fold and Thrust Belt - insight from  
1764 analog modeling. *Tectonics*, 30, TC2014, 1- 24, doi: 10.1029/2010TC002753.  
1765 [2011b](#).

1766

1767 Libak, A., Mjelde, R., Keers, H., Faleide, J. I. & Murai, Y., ~~2012~~: An intergrated  
1768 geophysical study of Vestbakken Volcanic Province, western Barents Sea  
1769 continental margin, and adjacent oceanic crust, *Marine Geophysical Research*,  
1770 33(2), 187-207, [2012a](#).

1771

1772 [Libak, A., Eide, C. H., Mjelde, R., Keers, H., and Flüh, E. R.: From pull-apart basins to  
1773 ultraslow spreading: Results from the western Barents Sea Margin.  
1774 \*Tectonophysics\*, 514-517, 44-61, 2012b.](#)

1775

1776 Lorenzo, J. M., ~~1997~~: Sheared continental margins: an overview, *Geo-Marine  
1777 Letters*, 17(1), 1-3, [1997](#).

1778

1779 Lowell, J. D., ~~1972~~: Spitsbergen Tertiary orogenic belt and the Spitsbergen fracture  
1780 zone, *Geol. Soc. Am. Bull.*, 83, 3091-3102, doi:10.1130/0016-  
1781 7606(1972)83[3091:STOBAT]2.0.CO;2, [1972](#).

1782

1783 Lundin, E. R. & Doré, A. G., ~~1997~~: A tectonic model for the Norwegian passive  
1784 margin with implications for the NE Atlantic.: Early Cretaceous to break-up.  
1785 *Journal of the Geological Society London*, 154, 545-550, [1997](#).

1786

1787 Lundin, E. R., Doré, A. G., Rønning, K. & Kyrkjebø, R., ~~2013~~: Repeated inversion  
1788 in the Late Cretaceous-Cenozoic northern Vøring Basin, offshore Norway,  
1789 *Petroleum Geoscience*, 19(4), 329-341, [2013](#).

1790

1791 Luth, S., Willingshofer, E., Sokoutis, D. & Cloetingh, S., ~~2010~~: ~~a~~Analogue  
1792 modelling of continental collision: Influence of plate coupling on mantle  
1793 lithosphere subduction, crustal deformation and surface topography,  
1794 *Tectonophysics*, 4184, 87-102, doi: 10.1016/j.tecto2009.08.043, [2010](#).

1795

1796 Maher, H. D., Jr., ~~S~~-Bergh, ~~S~~, ~~A~~-Braathen, ~~A~~, and ~~Y~~-Ohta, ~~Y~~, ~~1997~~: Svartfjella,  
1797 Eidembukta, and Daudmannsodden lineament: Tertiary orogen-parallel motion in  
1798 the crystalline hinterland of Spitsbergen's fold-thrust belt, *Tectonics*, 16(1), 88-  
1799 106, doi:10.1029/96TC02616, [1997](#).

1800

1801 Mandl, G., de Jong, L. N. J., and Maltha, A., ~~1977~~: Shear zones in granular material.  
1802 *Rock Mechanics*, 9, 95-144, [1977](#).

1803

1804 Manduit, T. & Dauteuil, O., ~~1996~~: Small scale modeling of oceanic transform  
1805 zones, *Journal of Geophysical Research*, 101(B9), 20195-20209, [1996](#).

1806

1807 Mann, P., ~~2007~~: Global catalogue, classification and tectonic origins of restraining

Formatted: Font: +Body (Cambria)

1804 and releasing bends on active and ancient strike-slip fault systems. *in*:  
1805 Cunningham,W.D. & Mann,P. (eds.), 2007: Tectonics of Strike-Slip Restraining and  
1806 Releasing Bends, Geological Society London Special Publication, 290, 13-142,  
1807 [2007](#).  
1808  
1809 Mann,P., Hempton,M.R., Bradley,D.C., & Burke,K.,[1983](#): Development of pull-  
1810 apart basins. *Journal of Geology*, 91(5), 529-554,[1983](#).  
1811  
1812 Mascle,J. & Blarez,E.,[1987](#): Evidence for transform margin evolution from the  
1813 Ivory Coast Ghana continental margin, *Nature*, 326, 378-381,[1987](#).  
1814  
1815 McClay,K.R.,[1990](#): Extensional fault systems in sedimentary basins. A review of  
1816 analogue model studies, *Marine and Petroleum Geology*, 7, 206-233,[1990](#).  
1817  
1818 Mitra,S.,[1993](#): Geometry and kinematic evolution of inversion structures.  
1819 *American Association of Petroleum Geologists Bulletin*, 77, 1159-1191,[1993](#).  
1820  
1821 Mitra,S. & Paul,D.,[2011](#): Structural geology and evolution of releasing and  
1822 constraining bends: Insights from laser-scanned experimental models,  
1823 *American Association of Petroleum Geologists Bulletin*, 95(7), 1147-1180,[2011](#).  
1824  
1825 Morgenstern,N.R. & Tchalenko,J.S.,[1967](#): Microscopic structures in kaolin  
1826 subjected to direct shear, *Géotechnique*, 17, 309-328,[1967](#).  
1827  
1828 Mosar,J., Torsvik,T.H., & the BAT Team,[2002](#): Opening of the Norwegian and  
1829 Greenland Seas: Plate tectonics in mid Norway since the late Permian. in: E.Eide  
1830 (ed.): *BATLAS. Mid Norwegian plate reconstruction atlas with global and Atlantic*  
1831 *perspectives*. Geological Survey of Norway, 48-59,[2002](#).  
1832  
1833 Mouslopoulou,V., Nicol,A., Little,T.A., & Walsh,J.J.,[2007](#): Terminations of  
1834 large-strike-slip faults: an alternative model from New Zealand, in:  
1835 Cunningham,W.D. & Mann,P. (eds.): *Tectonics of Strike-Slip Restraining and*  
1836 *Releasing Bends*, Geological Society London Special Publication, 290, 387- 415,  
1837 [2007](#).  
1838  
1839 Mouslopoulou,V., Nicol,A., Walsh,J.J., Beetham,D., & Stagpoole,V.,[2008](#):  
1840 Quaternary temporal stability of a regional strike-slip and rift fault interaction.  
1841 *Journal of Structural Geology*, 30, 451-463,[2008](#).  
1842  
1843 Myhre,A.M. & Eldholm,O.,[1988](#): The western Svalbard margin (74-80°N).  
1844 *Marine and Petroleum Geology*, 5, 134-156,[1988](#).  
1845  
1846 Myhre,A.M., Eldholm,O., & Sundvor,E.,[1982](#): The margin between Senja and  
1847 Spitsbergen Fracture Zones: Implications from plate tectonics. *Tectonophysics*,  
1848 89, 33-50,[1982](#).  
1849  
1850 Naylor,M.A., Mandl,G., & Sijpestijn,C.H.K.,[1986](#): Fault geometries in  
1851 basement-induced wrench faulting under different initial stress states. *Journal of*  
1852 *Structural Geology*, 8, 737-752,[1986](#).

1853 Nemcok, M., Rybár, S., Sinha, S.T., Hermeston, S.A. & Ledvényiová, L., 2016:  
1854 Transform margins: development, controls and petroleum systems – an  
1855 introduction. in: Nemcok, M., Rybár, S., Sinha, S.T., Hermeston, S.A. & Ledvényiová, L.  
1856 (eds.): Transform Margins;: Development, Control and Petroleum Systems,  
1857 Geological Society London, Special Publication, 431, 1-38, 2016.  
1858  
1859  
1860 Odonne, F. & Vialon, P., 1983: Analogue models of folds above a wrench fault,  
1861 Tectonophysics, 990, 31-46, 1983.  
1862  
1863 Pace, P. & Calamita, F., 2014: Push-up inversion structures v. fault-bend  
1864 reactivation anticlines along oblique thrust ramps: examples from the Apennines  
1865 fold-and-thrust-belt, Italy, Journal Geological Society London, 171, 227-238, 2014.  
1866  
1867 Pascal, C. & Gabrielsen, R. H., 2001: Numerical modelling of Cenozoic stress  
1868 patterns in the mid Norwegian Margin and the northern North Sea. Tectonics,  
1869 20(4), 585-599, 2001.  
1870  
1871 Pascal, C., Roberts, D., & Gabrielsen, R. H., 2005: Quantification of neotectonic  
1872 stress orientations and magnitudes from field observations in Finnmark, northern  
1873 Norway. Journal of Structural Geology, 27, 859-870, 2005.  
1874  
1875 Peacock, D. C. P., Nixon, C. W., Rotevatn, A., Sanderson, D. J., & Zuluaga, L. F.,  
1876 2016: Glossary of fault and other fracture networks, Journal of Structural Geology,  
1877 92, 12-29, doi: 10.1016/j.jgs.2016.09.008, 2016.  
1878  
1879 Perez-Garcia, C., Safranova, P. A., Mienert, J., Berndt, C., & Andreassen, K., 2013:  
1880 Extensional rise and fall of a salt diapir in the Sørvestsnaget Basin, SW Barents Sea.  
1881 Marine and Petroleum Geology, 46, 129-134, 2013.  
1882  
1883 Planke, S., Alvestad, E., and Eldholm, O., 1999; Seismic characteristics of  
1884 basaltic extrusive and intrusive rocks: The Leading Edge, 18(3), 342-348.  
1885 <https://doi-org.ezproxy.uio.no/10.1190/1.1438289>, 1999.  
1886  
1887 Ramberg, H., 1967: Gravity, deformation and the Earth's crust, Academic Press,  
1888 New York, 214pp, 1967.  
1889  
1890 Ramberg, H., 1981: Gravity, deformation and the Earth's crust, 2nd edition.  
1891 Academic Press, New York 452pp, 1981.  
1892  
1893 Ramsay, J. G. & Huber, M. I., 1987: The techniques of modern structural  
1894 geology. Vol. 2: Folds and fractures. Academic Press, London, 309-700, 1987.  
1895  
1896 Reemst, P., Cloetingh, S., & Fanavoll, S., 1994: Tectonostratigraphic modelling  
1897 of Cenozoic uplift and erosion in the south-western Barents Sea. Marine and  
1898 Petroleum Geology, 11, 478-490, 1994.  
1899

1900 Richard, P. D., Ballard, B., Colletta, B. & Cobbold, P. R., 1989: Naissance et  
1901 evolution de failles au dessus d'un décrochement de socle: Modelisation  
1902 experimental et tomographie, C. R. Acad.Sci. Paris, 308,9, 2111-2118, 1989.  
1903  
1904 Richard, P. D. & Cobbold, P. R., 1989: Structures et fleur positives et  
1905 décrochements crustaux: mdélisation analogique et interpretation mechanique,  
1906 C.R.Acad.Sci.Paris, 308, 553-560, 1989.  
1907  
1908 Richard, P. & Krantz, R. W., 1991: Experiments on fault reactivation in strike-  
1909 slip mode, Tectonophysics, 188, 117-131, 1991.  
1910  
1911 Richard, P., Mocquet, B. & Cobbold, P. R., 1991: Experiments on simultaneous  
1912 faulting and folding above a basement wrench fault, Tectonophysics, 188, 133-  
1913 141, 1991.  
1914  
1915 Riedel, W., 1929: Zur Mechanik geologischer Brucherscheinungen. Centralblatt für  
1916 Mineralogie, Geologie und Palentologie, 1929B, 354-368, 1929.  
1917  
1918 Riis, F., Vollset, J. & Sand, M., 1986: Tectonic development of the western  
1919 margin of the Barents Sea and adjacent areas. in: M.T.Halbouty (ed.): Future  
1920 petroleum provinces of the World. American Association of Petroleum Geologists  
1921 Memoir, 40, 661-667, 1986.  
1922  
1923 Roberts, D.G., 1989: Basin inversion in and around the British Isles, in: M.A.Cooper  
1924 & G.D.Williams (eds.): Inversion Tectonics. Geological Society of London Special  
1925 Publication, 44, 131-150, 1989.  
1926  
1927 Ryseth, A., Augustson, J. H., Charnock, M., Haugrud, O., Knutsen, S.-M., Midbøe, P.  
1928 S., Opsal, J. G. & Sundsbø, G., 2003: Cenozoic stratigraphy and evolution of the  
1929 Sørvestsnaget Basin, southwestern Barents Sea. Norwegian Journal of Geology, 83,  
1930 107-130, 2003.  
1931  
1932 Saunders, A. D., Fitton, J. G., Kerr, A. C., Norry, M. J., and Kent, R. W., 1997: The  
1933 North Atlantic Igneous Province: Geophysical Monograph 100, American  
Geophysical Union, pp. 45-93, 1997.  
1934  
1935 Scheurs, G., 1990: Experiments on strike-slip faulting and block rotation, *Geology*,  
1936 22,567-570, 1990.  
1937  
1938 Schreurs, G., 2003: Fault development and interaction in distributed strike-slip  
1939 shear zones: an experimental approach. in: Storti, F., Holdsworth, R.E. & Salvini, F.  
1940 (eds): Intraplate Strike-slip Deformation Belts, Geological Society of London  
Special Publication, 210, 35-82, 2003.  
1941  
1942 Schreurs, G., Colletta, B., 1998: Analogue modelling of faulting in zones of  
1943 continental transpression and transtension. in: Holdsworth, R.E., Strachan, R.A.,  
1944 Dewey, J.F. (eds.), Continental Transpressional and Transtensional Tectonics,  
1945 Geological Society of London Special Publication, London, 135, 59-79, 1998.  
1946

1947 Schreurs, G. & Colletta, B., 2003: Analogue modelling of continental  
1948 transpression and transtension. *in*: Scellart, W.P. & Passchier, C. (eds.): Analogue  
1949 Modelling of Large-scale Tectonic Processes. *Journal of the Virtual Explorer*, 7,  
1950 103-114, 2003.

1951

1952 Seiler, C., Fletcher, J. M., Quigley, M. C., Gleadow, A. J. & Kohn, B. P., 2010:  
1953 Neogene structural evolution of the Sierra San Felipe, Baja California: evidence of  
1954 proto-gulf transtension in the Gulf Extensional Province? *Tectonophysics*, 488(1),  
1955 87-109, 2010.

1956

1957 Sims, D., Ferrill, D. A., & Stamatakos, J. A., 1999: Role of a brittle décollement in  
1958 the development of pull-apart basins : experimental results and natural examples.  
1959 *Journal of Structural Geology*, 21, 533-554, 1999.

1960

1961 Sokoutis, D., 1987: Finite strain effects in experimental mullions. *Journal of*  
1962 *Structural Geology*, 9, 233-249, 1987.

1963

1964 Stearns, D. W., 1978: Faulting and forced folding in the Rocky Mountains Foreland,  
1965 *Geological Society of America Memoir*, 151, 1-38, 1978.

1966

1967 Sylvester, A. G. (ed); 1985: Wrench Fault Tectonics, Selected papers reprinted  
1968 from the AAPG Bulletin and other geological journals, American Association of  
1969 Petroleum Geologists Reprint Series 28, 3 74pp, 1985.

1970

1971 Sylvester, A. G., 1988: Strike-slip faults. *Geological Society of America Bulletin*, 100,  
1972 1666-1703, 1988.

1973

1974 Talwani, M. & Eldholm, O., 1977: Evolution of the Norwegian-Greenland Sea.  
1975 *Geological Society of America Bulletin*, 88, 969-999, 1977.

1976

1977 Tchalenko, J. S., 1970: Similarities between shear zones of different magnitudes.  
1978 *Geological Society of America Bulletin*, 81, 1625-1640, 1970.

1979

1980 Tron, V. & Brun, J.-P., 1991: Experiments on oblique rifting in brittle-ductile  
1981 systems. *Tectonophysics*, 188(1/2), 71-84, 1991.

1982

1983 [Tsikalas, F., Faleide, J. I., Eldholm, O., and Blaiçh, O. A.: The NE Atlantic conjugate](#)  
1984 [Margins. In: Roberts, D.G. & Bally, A.W., Phanerozoic Passive Margins. Cratonic](#)  
1985 [Basins and Global Tectonic Maps, Elsevier, DOI: 10.1016/B978-0-444-56357-](#)  
1986 [6.00004-4, 2012.](#)

1987

1988 Twiss, R. J. & Moores, E. M., 2007: *Structural Geology*, 2nd Edition,  
1989 W.H. Freeman & Co., New York, 736pp, 2007.

1990

1991 Ueta, K., Tani, K. & Kato, T., 2000: Computerized X-ray tomography analysis of  
three-dimensional fault geometries in basement-induced wrench faulting,  
*Engineering Geology*, 56, 197-210, 2000.

Formatted: Font: +Body (Cambria)

Formatted: Font: +Body (Cambria)

1992 Uliana, M. A., Arteaga, M. E., Legarreta, L., Cerdan, J.J. & Peroni, G. O., 1995:  
1993 Inversion structures and hydrocarbon occurrence in Argentina. *in*: Buchanan, J.G. &  
1994 Buchanan, P.G. (eds.): Basin Inversion, Geological Society London Special  
1995 Publication, 88, 211-233, 1995.

1996  
1997 Vågnes, E., 1997: Uplift at thermo-mechanically coupled ocean-continent  
1998 transforms: modeled at the Senja Fracture Zone, southwestern Barents Sea. *Geo-*  
1999 *Marine Letters*, 17, 100-109, 1997.

2000 Vågnes, E., Gabrielsen, R. H., & Haremo, P., 1998: Late Cretaceous-Cenozoic  
2001 intraplate contractional deformation at the Norwegian continental shelf: timing,  
2002 magnitude and regional implications. *Tectonophysics*, 300, 29-46, 1998.

2003 Weijermars, R., and Schmeling, H., 1986: Scaling of Newtonian and non-  
2004 Newtonian fluid dynamics without inertia for quantitative modelling of rock flow  
2005 due to gravity (including the concept of rheological similarity. *Physics of the Earth*  
2006 *and Planetary Interiors*, 43, 316-330, 1986.

2007 Wilcox, R. E., Harding, T. P., & Selly, D. R., 1973: Basic wrench tectonics.  
2008 *American Association of Petroleum Geologists Bulletin*, 57, 74-69, 1973.

2009  
2010 Williams, G. D., Powell, C. M., & Cooper, M. A., 1989: Geometry and kinematics  
2011 of inversion tectonics. *in*: M.A.Cooper & G.D.Williams (eds.): *Inversion Tectonics*.  
2012 *Geological Society of London Special Publication*, 44, 3-16, 1989.

2013  
2014 Willingshofer, E., Sokoutis, D., & Burg, J.-P., 2005: Lithosphere-scale analogue  
2015 modelling of collision zones with a pre-existing weak zone, *in*: Gapais, D.,  
2016 Brun, J.P. & Cobbold, P.R. (eds.): *Deformation Mechanisms, Rheology and Tectonics*:  
2017 *from Minerals to the Lithosphere*, Geological Society London Special  
2018 *Publication*, 43, 277-294, 2005.

2019  
2020 Willingshofer, E., Sokoutis, D., Beekman, Schönebeck, F., Warsitzka, J.-M., Michael,  
2021 M., & Rosenau, M., 2018: Ring shear test data of feldspar sand and quartz sand  
2022 used in the Tectonic Laboratory (TecLab) at Utrecht University for experimental  
2023 Earth Science applications. V. 1. GFZ Data Service.  
2024 <https://doi.org/10.5880/idgeo.2018.072>, 2018.

2025  
2026 Woodcock, N. H. & Fisher, M., 1986: Strike-slip duplexes. *Journal of Structural*  
2027 *Geology*, 8(7), 725-735, 1986.

2028  
2029 Woodcock, N. H. & Schubert, C., 1994: Continental strike-slip tectonics. *in*:  
2030 P.L.Hancock (ed.): *Continental Deformation* (Pergamon Press), 251-263, 1994.

2031  
2032 Yamada, Y. & McClay, K. R., 2004: Analog modeling of inversion thrust  
2033 structures, experiments of 3D inversion structures above listric fault systems, *in*:  
2034 McClay, K.R. (ed.): *Thrust Tectonics and Petroleum Systems*, American Association  
2035 *of Petroleum Geologists Memoir*, 82, 276-302, 2004.

2036  
2037

Formatted: Font: +Body (Cambria)